



# User's Manual for Data for Validating Models for PV Module Performance

W. Marion, A. Anderberg, C. Deline, S. Glick,  
M. Muller, G. Perrin, J. Rodriguez, S. Rummel,  
K. Terwilliger, and T.J. Silverman

**NREL is a national laboratory of the U.S. Department of Energy  
Office of Energy Efficiency & Renewable Energy  
Operated by the Alliance for Sustainable Energy, LLC**

This report is available at no cost from the National Renewable Energy  
Laboratory (NREL) at [www.nrel.gov/publications](http://www.nrel.gov/publications).

**Technical Report**  
NREL/TP-5200-61610  
April 2014

Contract No. DE-AC36-08GO28308

# User's Manual for Data for Validating Models for PV Module Performance

W. Marion, A. Anderberg, C. Deline, S. Glick,  
M. Muller, G. Perrin, J. Rodriguez,  
S. Rummel, K. Terwilliger, and T.J. Silverman

Prepared under Task No. SS13.4010

**NREL is a national laboratory of the U.S. Department of Energy  
Office of Energy Efficiency & Renewable Energy  
Operated by the Alliance for Sustainable Energy, LLC**

This report is available at no cost from the National Renewable Energy  
Laboratory (NREL) at [www.nrel.gov/publications](http://www.nrel.gov/publications).

## NOTICE

This report was prepared as an account of work sponsored by an agency of the United States government. Neither the United States government nor any agency thereof, nor any of their employees, makes any warranty, express or implied, or assumes any legal liability or responsibility for the accuracy, completeness, or usefulness of any information, apparatus, product, or process disclosed, or represents that its use would not infringe privately owned rights. Reference herein to any specific commercial product, process, or service by trade name, trademark, manufacturer, or otherwise does not necessarily constitute or imply its endorsement, recommendation, or favoring by the United States government or any agency thereof. The views and opinions of authors expressed herein do not necessarily state or reflect those of the United States government or any agency thereof.

This report is available at no cost from the National Renewable Energy Laboratory (NREL) at [www.nrel.gov/publications](http://www.nrel.gov/publications).

Available electronically at <http://www.osti.gov/scitech>

Available for a processing fee to U.S. Department of Energy and its contractors, in paper, from:

U.S. Department of Energy  
Office of Scientific and Technical Information  
P.O. Box 62  
Oak Ridge, TN 37831-0062  
phone: 865.576.8401  
fax: 865.576.5728  
email: <mailto:reports@adonis.osti.gov>

Available for sale to the public, in paper, from:

U.S. Department of Commerce  
National Technical Information Service  
5285 Port Royal Road  
Springfield, VA 22161  
phone: 800.553.6847  
fax: 703.605.6900  
email: [orders@ntis.fedworld.gov](mailto:orders@ntis.fedworld.gov)  
online ordering: <http://www.ntis.gov/help/ordermethods.aspx>

*Cover Photos: (left to right) photo by Pat Corkery, NREL 16416, photo from SunEdison, NREL 17423, photo by Pat Corkery, NREL 16560, photo by Dennis Schroeder, NREL 17613, photo by Dean Armstrong, NREL 17436, photo by Pat Corkery, NREL 17721.*



Printed on paper containing at least 50% wastepaper, including 10% post consumer waste.

## Preface

This user's manual describes performance data measured for flat-plate photovoltaic (PV) modules installed in Cocoa, Florida; Eugene, Oregon; and Golden, Colorado. The data include PV module current-voltage curves and associated meteorological data for approximately one-year periods. These publicly available data are intended to facilitate the validation of existing models for predicting the performance of PV modules and for the development of new and improved models. For comparing different modeling approaches, using these public data will provide transparency and more meaningful comparisons of the relative benefits.

The data sets and this manual were produced by the National Renewable Energy Laboratory under the Systems Integration Subprogram, which is funded and monitored by the U.S. Department of Energy's Office of Energy Efficiency and Renewable Energy.

## Acknowledgments

This work was supported by the U.S. Department of Energy under Contract No. DE-AC36-08-GO28308 with the National Renewable Energy Laboratory (NREL). The work began in 2010 and concluded in 2014 as a part of the Emerging Technology Characterization agreement. The authors are thankful for the efforts of the Department of Energy technical managers who supported this work: Mike Cliggett, Holly Thomas, and Guohui Yuan.

The authors are thankful for the efforts of Joe del Cueto for his work at NREL in initiating the PV module deployments, and for the efforts of the following individuals and organizations: Stephen Barkaszi and Mark Jacobs (Florida Solar Energy Center), who operated the PV module test facility in Cocoa, Florida; Frank Vignola, Rich Kessler, and Josh Peterson (University of Oregon), who operated the PV module test facility in Eugene; Nick Riedel and Larry Pratt (CFV Solar Test Laboratory, Inc.), who performed PV module characterizations per IEC-61853-1; Bruce King (Sandia National Laboratories), who performed PV module characterizations per the Sandia array performance model method; and Aron Dobos (NREL) and Josh Stein (Sandia National Laboratories), who peer reviewed this user's manual.

## List of Acronyms

a-Si	amorphous silicon
CdTe	cadmium telluride
CIGS	copper indium gallium selenide
CSV	comma separated variables
FF	fill factor
FSEC	Florida Solar Energy Center
HIT	heterojunction with intrinsic thin-layer
$I_{dh}$	diffuse horizontal irradiance
$I_{dn}$	direct normal irradiance
IEC	International Electrotechnical Commission
$I_h$	global horizontal irradiance
$I_{mp}$	current of PV module in amperes when operating at maximum power
$I_{sc}$	short-circuit current of PV module in amperes
ISO	International Organization for Standardization
I-V	current-voltage
mPERT	mobile PERT
m-Si	multi-crystalline silicon
NREL	National Renewable Energy Laboratory
PERT	performance and energy rating testbed
$P_m$	maximum power of PV module in watts
POA	plane-of-array
PV	photovoltaic
QA	quality assessment
Sandia	Sandia National Laboratories
STC	standard test conditions
$V_{mp}$	voltage of PV module in volts when operating at maximum power
$V_{oc}$	open-circuit voltage of PV module in volts
x-Si	single-crystalline silicon

# Table of Contents

<b>List of Acronyms</b> .....	<b>v</b>
<b>List of Figures</b> .....	<b>vii</b>
<b>List of Tables</b> .....	<b>vii</b>
<b>1 Introduction</b> .....	<b>1</b>
1.1 PV Technologies.....	1
1.2 Participating Organizations and Roles.....	2
<b>2 Data Measurement</b> .....	<b>3</b>
2.1 Equipment.....	3
2.2 Station Operations.....	5
2.3 Quality Assessment.....	5
<b>3 Data and Format</b> .....	<b>7</b>
3.1 File Convention.....	7
3.2 File Format.....	8
3.2.1 File Header.....	8
3.2.2 File Data.....	8
3.2.3 Missing Data .....	11
3.2.4 Solar Quality Assessment Residual .....	12
3.2.5 PV Module Soiling Derate.....	12
3.2.6 Daily Maintenance Start and End Times and Precipitation .....	13
3.2.7 Reading Data.....	13
<b>4 Characterization Data for PV Model Inputs</b> .....	<b>14</b>
<b>5 Performance Changes from Deployments</b> .....	<b>15</b>
<b>References</b> .....	<b>18</b>
<b>Appendix A – Quality Assessment Methods</b> .....	<b>19</b>
<b>Appendix B – Measurement Uncertainty Analysis</b> .....	<b>23</b>
<b>Appendix C – Sample Read Statements</b> .....	<b>38</b>

## List of Figures

Figure 2-1. PV module and equipment deployment at the FSEC, Cocoa, Florida.....	4
Figure 2-2. PV module and equipment deployment at the University of Oregon, Eugene, Oregon .....	4
Figure 2-3. PV modules deployed on the PERT at NREL, Golden, Colorado .....	5
Figure 2-4. Daily maintenance log sheet for the week of October 28, 2013, for the Eugene site .....	6
Figure B-1. I-V curve for representative PV module .....	26
Figure B-2. a) Type-B standard uncertainty vs. zenith angle for horizontally mounted CM22 (serial # 100163). b) Instrument responsivity ( $\mu\text{V} / \text{Wcm}^{-2}$ ) vs. incidence angle (degrees) (serial # 100163) .....	31
Figure B-3. Directional error for Kipp & Zonen CMP11 – CMP22 pyranometers [10] .....	32
Figure B-4. Typical temperature dependence of CM22 pyranometer .....	33
Figure B-5. Temperature uncertainty ( $^{\circ}\text{C}$ ) of outdoor ambient temperature sensor .....	35
Figure B-6. Third-order polynomial fit to outdoor ambient temperature uncertainty .....	35

## List of Tables

Table 2-1. List of NREL-Furnished Sensors and Data Acquisition Equipment .....	3
Table 3-1. File Names Corresponding to the PV Modules and Their Deployment Sites .....	7
Table 3-2. File Header Elements and Definitions (Line 2) .....	8
Table 3-3. File Data Elements and Definitions (for all except the first three lines) .....	9
Table 5-1. PV Module Changes in Derived Performance Ratings from Start to End of Deployments .....	17
Table B-1. Summary of Standard Uncertainty Components .....	24

# 1 Introduction

This user's manual describes a comprehensive data set of current-voltage (I-V) curves and associated meteorological data for photovoltaic (PV) modules representing all flat-plate PV technologies and for three different locations and climates for approximately one-year periods. The data measurement locations were Cocoa, Florida (subtropical climate); Eugene, Oregon (marine west coast climate); and Golden, Colorado (semi-arid climate). These publicly available data are intended to facilitate the validation of existing models for predicting the performance of PV modules and for the development of new and improved models.

The data include a wide range of irradiance and temperature conditions representing each season for each location. The data are not meant to be serially complete because quality assessment (QA) procedures removed data for conditions when measurements would provide unreliable data, such as irradiance changes during the I-V curve measurement and the presence of snow or ice on the PV modules.

The data include the following periods:

- Cocoa – January 21, 2011, through March 4, 2012
- Golden – August 14, 2012, through September 24, 2013
- Eugene – December 20, 2012, through January 20, 2014.

The PV modules tested were an assortment of PV modules that the National Renewable Energy Laboratory (NREL) had tested previously and new PV modules purchased for this work. During the measurement periods, the performance of some PV modules degraded more than the performance of others. This should be considered when using the data for model validations and is discussed in Section 5.

## 1.1 PV Technologies

The PV modules tested were for PV technologies available in 2010, when the work effort began. They include:

- Single-crystalline silicon (x-Si) PV modules
- Multi-crystalline silicon (m-Si) PV modules
- Cadmium telluride (CdTe) PV modules
- Copper indium gallium selenide (CIGS) PV modules
- Amorphous silicon (a-Si) tandem and triple junction PV modules
- Amorphous silicon/crystalline silicon or heterojunction with intrinsic thin-layer (HIT) PV modules
- Amorphous silicon/microcrystalline silicon PV modules.

Even though the market share for a-Si tandem and triple PV modules has decreased dramatically since this work began, their large sensitivity to the solar spectrum makes their data useful for validating the robustness of models that account for the effects of variations in the solar spectrum

on PV module performance. Because spectral effects directly impact the PV module short-circuit current, the use of I-V curve data is particularly well suited for evaluating models of this type.

## 1.2 Participating Organizations and Roles

For one of the locations and climates, NREL performed I-V curve and meteorological data measurements at its location in Golden. Other measurement locations were Cocoa, with the measurements performed by the Florida Solar Energy Center (FSEC), and Eugene, with the measurements performed by the University of Oregon. The FSEC and the University of Oregon were selected to perform measurements as a result of a competitive solicitation, with the qualitative merit associated with experience and capability and for additional factors related to the diversity of their climate from NREL's. Climate diversity was judged with respect to dry bulb temperature, cloudiness, atmospheric water vapor, atmospheric aerosols, latitude, and elevation. These factors all influence the performance of PV modules; the measured data for the three locations provide climatic diversity for evaluating the sensitivity of PV module models to climate.

As a check on the integrity of the measurements and PV modules, NREL performed indoor performance measurements at standard test conditions (STC) for each PV module before and after deployment in the field. After deployment, more extensive measurements were performed to provide data for determining parameters and coefficients for use as inputs to potential models undergoing model validation. CFV Solar Test Laboratory, Albuquerque, New Mexico, measured the irradiance-temperature characteristics per International Electrotechnical Commission (IEC) Standard 61853 [1] and the temperature coefficients per IEC 61215 [2] or IEC 61646 [3]. Sandia National Laboratories (Sandia) measured coefficients and parameters for use with the Sandia PV array performance model [4].

## 2 Data Measurement

Measurement equipment was selected to provide low measurement errors, station operations were followed to ensure equipment operated properly, and QA methods were implemented to exclude data not meeting quality thresholds.

### 2.1 Equipment

NREL provided the equipment for measurements at the Cocoa and Eugene sites. The equipment was transported to the sites in a shipping container, and then the shipping container was used as an integral part of the test facility. Structure was attached to the shipping container for deploying the PV modules, and the roof was used for locating the solar radiation and other meteorological sensors. Data acquisition equipment was located inside the shipping container in a temperature-controlled environment. The sensors and data acquisition equipment are listed in Table 2-1. Equipment was selected to provide low measurement errors, with special attention paid to the selection of the solar radiation instrumentation, which is usually the largest source of error when measuring the performance of PV modules or systems.

Figures 2-1 and 2-2 depict the test facility deployments at the Cocoa and Eugene sites. The same set of equipment and PV modules was deployed at the two sites. The deployment at the Cocoa site began in January 2011 and ended in March 2012. The deployment at the Eugene site began in December 2012 and ended in January 2014. After each deployment ended, the shipping container with equipment was returned to NREL, where the solar radiation and meteorological sensors were recalibrated and the performance of the PV modules was retested at STC with a solar simulator.

**Table 2-1. List of NREL-Furnished Sensors and Data Acquisition Equipment**

Item	Parameter	Instrument
1	Wind Speed/Wind Direction/ Precipitation/Temperature/ Relative Humidity/Barometric Pressure	Vaisala WXT520 Weather Sensor
2	Direct Normal Irradiance	Kipp & Zonen CHP1 pyrhelimeter
3	Global Horizontal Irradiance	Kipp & Zonen CMP 22 pyranometer
4	Diffuse Horizontal Irradiance	Kipp & Zonen CMP 22 pyranometer
5	Plane-of-Array Irradiance	Kipp & Zonen CMP 22 pyranometer
6	Plane-of-Array Irradiance	LI-COR pyranometer
7	Solar Tracker	Kipp & Zonen Model SOLYS 2
8	Data Logger	Campbell Scientific, Inc. Model CR1000
9	Data Logger Communications	RAVEN XE-EVDO (Verizon network)
10	PV Module I-V Curve	Daystar MT5 Multi-Tracer
11	PV Module Back-Surface Temperature	Omega Model CO1-T Style I Thermocouple



**Figure 2-1. PV module and equipment deployment at the FSEC, Cocoa, Florida**



**Figure 2-2. PV module and equipment deployment at the University of Oregon, Eugene, Oregon**

A second set of PV modules was deployed at NREL from August 2012 through September 2013. These PV modules were of the same manufacturers and models as the set of PV modules deployed in Florida and Oregon. Their performance was measured on NREL's performance and energy rating testbed (PERT) with the same type of equipment listed in Table 2-1. The PERT is located at NREL's Outdoor Test Facility building and has been measuring the performance of PV modules since 1996. Figure 2-3 shows PV modules installed on the roof of the Outdoor Test Facility.



**Figure 2-3. PV modules deployed on the PERT at NREL, Golden, Colorado**

## **2.2 Station Operations**

Station operations included daily, weekly, and monthly maintenance. Each day, except for weekends and holidays, the solar radiometers were cleaned, the solar tracker was checked for proper operation, and the PV module soiling amount was estimated. As a further measure of soiling, one (the reference PV module) of two identical PV modules was cleaned as a comparative measure against the one not cleaned. Figure 2-4 is an example maintenance log showing the daily maintenance activities. Weekly maintenance activities included checking radiometer desiccants and domes or windows and the electrical connectors and wiring. Monthly maintenance activities included checking the integrity of the PV module support structure and washing the PV modules if needed. PV modules were washed infrequently at all sites due to minimal soiling.

## **2.3 Quality Assessment**

NREL retrieved the data each day via the internet and archived it in a database. QA methods were implemented to exclude data not meeting quality thresholds from being included in data distributed outside of NREL; consequently, data files are not serially complete. The QA methods are based on those previously established to provide International Organization for Standardization (ISO) 17025 [5] accredited data for PV modules installed on the PERT at NREL. They include checks for the reasonableness of the I-V curves, irradiances, PV module temperatures, and meteorological data. The daily QA checks also facilitated identifying and resolving any operational problems in a timely manner. Appendix A provides a complete description of the QA methods.

**DAILY MAINTENANCE CHECKLIST**

For the Week 10 / 28 / 13 to 11 / 1 / 13

**Date and Time of Maintenance**

Day of Week	Sun	Mon	Tue	Wed	Thur	Fri	Sat
Month/Day/Year		10-28	10-29	10-30	10-31	11-1	
Begin Time (LST)		7:00	6:44	6:35	7:44	8:00	
End Time (LST)		7:07	6:47	6:39	7:47	8:02	
Operator's Initials		RK	RK	RK	JTP	JTP	

**Cleaning Instruments and Sensors**

Pyrheliometer		O	O	O	O	O	
Global Horizontal Pyranometer		O	O	O	O	O	
Diffuse Horizontal Pyranometer		O	O	O	O	O	
Kipp & Zonen Tilt Pyranometer		O	O	O	O	O	
LI-COR Tilt Pyranometer		O	O	O	O	O	
Reference PV Module		O	O	O	O	O	
WXT520 Weather Sensor		O	O	O	O	O	

Symbols: X = Bad Condition O = Good Condition

**Checking Solar Tracker Operation**

Bubble Level		O	O	O	O	O	
Tracker Movement		O	O	O	O	O	
Pyrheliometer Alignment		NA	NA	O	NA	NA	
Shading Ball Alignment		NA	NA	O *	NA	NA	

Symbols: X = Bad Condition O = Good Condition NA = No Alignment Check, too cloudy

**Weather Observation**

Sky Cloudiness		PC	C	C	O	O	
----------------	--	----	---	---	---	---	--

Symbols: C = Clear PC = Partly cloudy O = Overcast

**PV Module Surface Conditions**

Presence of Soiling or Snow		N	LS	N	LS	N	
-----------------------------	--	---	----	---	----	---	--

Symbols: N = None LS = Light Soiling MS = Medium Soiling HS = Heavy Soiling SN = Snow

**Enter comments to explain bad conditions, corrective actions and other events.**

C		Sensors		*At			
O		wet		4:17PM			
M							
M							
E							
N							
T							
S							

*Notify NREL immediately of any "X" conditions not corrected by daily maintenance.*

**Figure 2-4. Daily maintenance log sheet for the week of October 28, 2013, for the Eugene site**

## 3 Data and Format

This section of the user’s manual provides information on which files contain data for which PV modules and how the files are formatted.

### 3.1 File Convention

The files contain comma separated variables (CSV). The naming convention uses the deployment location and NREL PV module identifier as the file prefix, with the characters “csv” as the file extension. Table 3-1 lists the PV modules, the file name corresponding to their deployment, and pseudo manufacturer and model information for identifying PV modules of the same manufacturer and model installed at multiple locations.

**Table 3-1. File Names Corresponding to the PV Modules and Their Deployment Sites**

<b>NREL PV Module Identifier</b>	<b>Technology</b>	<b>Manufacturer/ Model</b>	<b>File Names</b>
<b>xSi12922</b>	Single-crystalline silicon	Manufacturer 1 Model A	Cocoa_xSi12922.csv Eugene_xSi12922.csv
<b>xSi11246</b>	Single-crystalline silicon	Manufacturer 1 Model A	Golden_xSi11246.csv
<b>mSi460A8</b>	Multi-crystalline silicon	Manufacturer 1 Model B	Cocoa_mSi460A8.csv Eugene_mSi460A8.csv
<b>mSi460BB</b>	Multi-crystalline silicon	Manufacturer 1 Model B	Golden_mSi460BB.csv
<b>mSi0166</b>	Multi-crystalline silicon	Manufacturer 2 Model C	Cocoa_mSi0166.csv Eugene_mSi0166.csv
<b>mSi0188</b>	Multi-crystalline silicon	Manufacturer 2 Model C	Cocoa_mSi0188.csv Eugene_mSi0188.csv
<b>mSi0247</b>	Multi-crystalline silicon	Manufacturer 2 Model C	Golden_mSi0247.csv
<b>mSi0251</b>	Multi-crystalline silicon	Manufacturer 2 Model C	Golden_mSi0251.csv
<b>CdTe75638</b>	Cadmium telluride	Manufacturer 3 Model D	Cocoa_CdTe75638.csv Eugene_CdTe75638.csv
<b>CdTe75669</b>	Cadmium telluride	Manufacturer 3 Model D	Golden_CdTe75669.csv
<b>CIGS39017</b>	Copper indium gallium selenide	Manufacturer 4 Model E	Cocoa_CIGS39017.csv Eugene_CIGS39017.csv
<b>CIGS39013</b>	Copper indium gallium selenide	Manufacturer 4 Model E	Golden_CIGS39013.csv
<b>CIGS8-001</b>	Copper indium gallium selenide	Manufacturer 5 Model F	Cocoa_CIGS8-001.csv Eugene_CIGS8-001.csv
<b>CIGS1-001</b>	Copper indium gallium selenide	Manufacturer 5 Model F	Golden_CIGS1-001.csv
<b>HIT05667</b>	Amorphous silicon/ crystalline silicon (HIT)	Manufacturer 6 Model G	Cocoa_HIT05667.csv Eugene_HIT05667.csv
<b>HIT05662</b>	Amorphous silicon/ crystalline silicon (HIT)	Manufacturer 6 Model G	Golden_HIT05662.csv
<b>aSiMicro03036</b>	Amorphous silicon/ microcrystalline silicon	Manufacturer 7 Model H	Cocoa_aSiMicro03036.csv Eugene_aSiMicro03036.csv
<b>aSiMicro03038</b>	Amorphous silicon/ microcrystalline silicon	Manufacturer 7 Model H	Golden_aSiMicro03038.csv

NREL PV Module Identifier	Technology	Manufacturer/ Model	File Names
aSiTandem72-46	Amorphous silicon tandem junction	Manufacturer 8 Model I	Cocoa_aSiTandem72-46.csv Eugene_aSiTandem72-46.csv
aSiTandem90-31	Amorphous silicon tandem junction	Manufacturer 8 Model I	Golden_aSiTandem90-31.csv
aSiTriple28324	Amorphous silicon triple junction	Manufacturer 9 Model J	Cocoa_aSiTriple28324.csv Eugene_aSiTriple28324.csv
aSiTriple28325	Amorphous silicon triple junction	Manufacturer 9 Model J	Golden_aSiTriple28325.csv

## 3.2 File Format

The data files consist of rows or lines of data. The data values within a line are separated by commas, which constitutes the CSV format. The CSV format is commonly used, and most software has built-in functions for reading or parsing it. When parsed, the line of data is broken into fields containing the values of the data elements.

### 3.2.1 File Header

The first two lines of data provide information about the PV module and the site location. The first line consists of nine fields containing text describing the header data values that are contained in line 2. Table 3-2 provides the field positions and header information contained in line 2.

**Table 3-2. File Header Elements and Definitions (Line 2)**

Field	Element	Description
1	PV Module Identifier	Unique alphanumeric module identifier assigned by NREL
2	City	City where measurement site located
3	State	State where measurement site located
4	Time Zone	Eastern = -5, Western = -7, Pacific = -8
5	Latitude	Latitude in decimal degrees, N+
6	Longitude	Longitude in decimal degrees, W-
7	Elevation	Elevation in meters above sea level
8	PV Module Tilt	PV module tilt angle from horizontal in degrees
9	PV Module Azimuth	PV module azimuth angle from north in degrees (N=0, E=90, S=180, W=270)

### 3.2.2 File Data

Line 3 consists of 42 fields and contains text describing the I-V curve and meteorological data contained in line 4 and subsequent lines. Table 3-3 provides the field positions and data information contained in the file beginning with line 4. Uncertainty values were assigned using the method outlined in Appendix B. Although measured, wind speed and direction are not

included because their instantaneous value at the time of the I-V curve does not correlate with PV module temperature because of the lag in PV module cooling or heating because of its thermal mass.

**Table 3-3. File Data Elements and Definitions (for all except the first three lines)**

<b>Field</b>	<b>Element</b>	<b>Description</b>
1	Date and Time	Local standard time for the site, formatted as yyyy-mm-ddThh:mm:ss
2	Plane-of-Array (POA) Irradiance	Amount of solar irradiance in watts per square meter received on the PV module surface at the time indicated, measured with CMP 22 pyranometer.
3	POA Irradiance Uncertainty	Uncertainty in percent based on random and bias error estimates.
4	PV Module Back-Surface Temperature	PV module back-surface temperature in degrees Celsius at the time indicated, measured behind center of cell near center of PV module.
5	PV Module Back-Surface Temperature Uncertainty	Uncertainty in degrees Celsius based on random and bias error estimates.
6	PV Module $I_{sc}$	Short-circuit current of PV module in amperes at the time indicated.
7	PV Module $I_{sc}$ Uncertainty	Uncertainty in percent based on random and bias error estimates.
8	PV Module $P_m$	Maximum power of PV module in watts at the time indicated.
9	PV Module $P_m$ Uncertainty	Uncertainty in percent based on random and bias error estimates.
10	PV Module $I_{mp}$	Current of PV module in amperes when operating at maximum power at the time indicated.
11	PV Module $I_{mp}$ Uncertainty	Uncertainty in percent based on random and bias error estimates.
12	PV Module $V_{mp}$	Voltage of PV module in volts when operating at maximum power at the time indicated.
13	PV Module $V_{mp}$ Uncertainty	Uncertainty in percent based on random and bias error estimates.
14	PV Module $V_{oc}$	Open-circuit voltage of PV module in volts at the time indicated.
15	PV Module $V_{oc}$ Uncertainty	Uncertainty in percent based on random and bias error estimates.
16	PV Module FF	Fill-factor of PV module in percent at the time indicated.
17	PV Module FF Uncertainty	Uncertainty in percent (relative) based on random and bias error estimates.

<b>Field</b>	<b>Element</b>	<b>Description</b>
18	Delta CMP 22 POA	Change in POA irradiance measured with CMP 22 pyranometer from the time indicated to the end of the I-V curve measurement (~1 second elapsed time).
19	Delta LI-COR POA	Change in POA irradiance measured with LI-COR pyranometer from the time indicated to the end of the I-V curve measurement (~1 second elapsed time).
20	MT5 Cabinet Temperature	Air temperature within cabinet containing the MT5 multi-tracer in degrees Celsius at the time indicated.
21	Dry Bulb Temperature	Dry bulb temperature at the site in degrees Celsius at the time indicated for Golden, nearest 5-second average to the time indicated for Cocoa and Eugene.
22	Dry Bulb Temperature Uncertainty	Uncertainty in degrees Celsius based on random and bias error estimates.
23	Relative Humidity	Relative humidity at the site in percent, nearest 5-second average to the time indicated.
24	Relative Humidity Uncertainty	Uncertainty in percent (relative) based on random and bias error estimates.
25	Atmospheric Pressure	Atmospheric pressure at the site in millibars, nearest 5-second average to the time indicated.
26	Atmospheric Pressure Uncertainty	Uncertainty in percent based on random and bias error estimates.
27	Precipitation	Accumulated daily total precipitation in millimeters at the time indicated.
28	Direct Normal Irradiance	Amount of solar irradiance in watts per square meter received within a 5.7° field-of-view centered on the sun, nearest 5-second average to the time indicated.
29	Direct Normal Irradiance Uncertainty	Uncertainty in percent based on random and bias error estimates.
30	Direct Normal Irradiance Standard Deviation	Standard deviation in watts per square meter of the 1-second samples in the 5-second average for the direct normal irradiance.
31	Global Horizontal Irradiance	Total amount of direct and diffuse solar irradiance in watts per square meter received on a horizontal surface, nearest 5-second average to the time indicated.
32	Global Horizontal Irradiance Uncertainty	Uncertainty in percent based on random and bias error estimates.
33	Global Horizontal Irradiance Standard Deviation	Standard deviation in watts per square meter of the 1-second samples in the 5-second average for the global horizontal irradiance.
34	Diffuse Horizontal Irradiance	Amount of solar irradiance in watts per square meter received from the sky (excluding the solar disk) on a horizontal surface, nearest 5-second average to the time indicated.

Field	Element	Description
35	Diffuse Horizontal Irradiance Uncertainty	Uncertainty in percent based on random and bias error estimates.
36	Diffuse Horizontal Irradiance Standard Deviation	Standard deviation in watts per square meter of the 1-second samples in the 5-second average for the diffuse horizontal irradiance.
37	Solar QA Residual	Residual of solar irradiance elements in watts per square meter determined by adding the diffuse horizontal irradiance to the product of the direct normal irradiance and the cosine of the zenith angle, and then subtracting the global horizontal irradiance. If in perfect agreement, the result is zero.
38	PV Module Soiling Derate	Normalized metric comparing daily performance of a PV module to an identical PV module that is cleaned during daily maintenance. Examples: 1.000 = no soiling loss, 0.980 = 2% soiling loss.
39	Daily Maintenance Start Time	Local standard time in HH:MM format when daily maintenance activities began. 99:99 = no daily maintenance.
40	Daily Maintenance End Time	Local standard time in HH:MM format when daily maintenance activities completed. 99:99 = no daily maintenance.
41	Precipitation Prior to Daily Maintenance	Accumulated daily total precipitation in millimeters prior to completion of the daily maintenance. If no daily maintenance, equals -9999.
42	I-V Curve Data Pairs	Integer N with value equal to the number of current-voltage pairs in the I-V curve. Varies by I-V curve.
43 to 43 + N - 1	I-V Curve I Values	N number of current values of the I-V curve, one per field.
43 + N to 43 + 2N - 1	I-V Curve V Values	N number of voltage values of the I-V curve, one per field, in same order as the I-V curve current values.

### 3.2.3 Missing Data

Data may be missing for fields 21 through 37. These fields are meteorological data measured with the Campbell Scientific data logger. Missing data are indicated by -9999. Data may be missing due to a failure to meet QA thresholds or equipment problems. For Golden, about 25% of the meteorological data are missing, primarily because of equipment downtime related to construction activities in the summer of 2013. Data measured with the Daystar MT5 multi-tracer (the I-V curves and fields 2 through 20) are always present for the times indicated in the data files (field 1), with the exception that uncertainty values may be coded missing for small measured values where a realistic uncertainty could not be determined. Data for times when measurements with the Daystar MT5 multi-tracer fail QA are not included in the files. The files are not intended to be serially complete. Data fields measured with the Daystar MT5 multi-tracer were considered essential; data fields measured with the Campbell Scientific data logger were considered supplemental. Because of the data logger program used with the Campbell data

logger for Golden, data for elements 30, 33, and 36 were not measured and are coded as missing (-9999) for all times for Golden.

### 3.2.4 Solar Quality Assessment Residual

The solar QA residual is a metric showing whether the measured values of direct normal irradiance ( $I_{dn}$ ), global horizontal irradiance ( $I_h$ ), and diffuse horizontal irradiance ( $I_{dh}$ ) comply with the equation that defines their relationship.

$$I_h = I_{dh} + I_{dn} \cdot \cos \theta_z \quad (1)$$

where:

$\theta_z$  = zenith angle, angle between a ray from the sun and the vertical.

The solar QA residual is defined by Eqn. 2

$$QA_{res} = I_{dh} + I_{dn} \cdot \cos \theta_z - I_h \quad (2)$$

If the value of the solar QA residual is zero, the measured values are in exact agreement with Eqn. 1. Values other than zero indicated departures (in watts per square meter) from Eqn. 1. A small value for the solar QA residual provides greater confidence in the measurement of the three irradiances. However, if two of the three irradiances are erroneous, the solar QA residual might still be small. For this work, a tracker aligned the  $I_{dn}$  instrument with the sun and moved a shading ball to block the sun's rays from reaching the  $I_{dh}$  instrument. If the tracker stops, the value of the measured  $I_{dn}$  becomes zero because the instrument is no longer aligned with the sun and the measured  $I_{dh}$  is essentially the same as the measured  $I_h$  because the shading ball no longer shades the  $I_{dh}$  instrument. Under this tracking failure scenario, the solar QA residual would be small, but misleading, if the direct normal irradiance is greater than zero.

For validation of models requiring direct normal and diffuse horizontal irradiances (such as angle-of-incidence models), users may want to perform an additional check of the consistency of the measurements by using the direct and diffuse irradiance measurements to model the plane-of-array (POA) irradiance and then compare it to the measured POA irradiance. Because it does not rely on a tracker, the measured POA irradiance is more reliable than the measured direct and diffuse irradiances, and as part of its QA, its measurements are checked with a redundant POA instrument.

### 3.2.5 PV Module Soiling Derate

PV module soiling derate values were determined by comparing the performance of two identical PV modules, one that was cleaned each work day and the other that was not cleaned. For the Cocoa and Eugene sites, PV module mSi0166 was cleaned, and its performance was compared to PV module mSi0188. For the Golden site, the PV module mSi0247 was cleaned, and its performance was compared to PV module mSi0251.

The PV module soiling derate values were determined by using the  $I_{sc}$  and irradiance values from the I-V curve data to calculate daily values of ampere-hours per kilowatt-hours per square meter POA irradiance. The daily values for the not-cleaned PV module were divided by those for

the cleaned PV module to estimate the PV module soiling derate value for that day. A value of 0.985 represents a soiling loss of 1.5%, and a value of 1.000 represents no soiling loss. Because PV modules mSi0166 and mSi0247 were cleaned each work day, their PV module soiling derate values are always equal to 1.000.

By analyzing the calculated PV module soiling derate values for days with no observed soiling indicated on the daily maintenance log sheets, we determined the 95% confidence interval of the method to be  $\pm 0.005$ . Consequently, calculated PV module soiling derate values greater than 0.995 were rounded to 1.000 (no soiling).

To ensure PV modules were not excessively dirty, rendering the data questionable, all the PV modules were cleaned if judged necessary. The PV modules at the Cocoa site were cleaned on February 28, 2011, and February 10, 2012, to remove primarily pollen. The PV modules at the Eugene site were cleaned on March 11, 2013; July 10, 2013; August 14, 2013; August 21, 2013; and August 26, 2013. At Eugene, no significant precipitation to help clean the PV modules occurred during July and August. The PV modules (except for mSi0247) at the Golden site were not manually cleaned, but the cleansing action of snow and rain kept the soiling loss to reasonable levels.

For the Cocoa site, the average daily PV module soiling derate was 0.999 and the minimum was 0.985. For the Eugene site, the average daily PV module soiling derate was 0.997 and the minimum was 0.964. For the Golden site, the average daily PV module soiling derate was 0.997 and the minimum was 0.977.

### **3.2.6 Daily Maintenance Start and End Times and Precipitation**

Daily maintenance included removing soiling and moisture in the form of dew or rain droplets from the pyranometers, pyrliometer, and the PV module that was regularly cleaned. Although the amount of soiling occurring since the last maintenance is likely not significant, we have observed that moisture on pyranometer domes and pyrliometer windows does cause measurement errors and impacts model results.

For best quality data, users may elect to not use data prior to the maintenance times if the Precipitation Prior to Daily Maintenance (field 41) is greater than zero, or almost any day for the Cocoa site with its high relative humidity and nighttime dew formation. Similarly, the data may be lower quality after the maintenance time if rain occurs during the day, as indicated by the Precipitation (field 27) being greater than the Precipitation Prior to Daily Maintenance (field 41).

For non-work days with no maintenance performed, it would be prudent to exclude data if Precipitation (field 27) indicated rainfall within the last few hours, and also for the first few daytime hours for the Cocoa site to permit the dew to evaporate from the pyranometer domes and pyrliometer window. Days without maintenance are indicated with the maintenance start and end times coded as 99:99 and the Precipitation Prior to Daily Maintenance coded as -9999.

### **3.2.7 Reading Data**

The files may be read with software compatible with the CSV format. Code snippets are included in Appendix C to demonstrate reading data lines with a variable number of fields. The number of fields in a line of data varies because the number of current-voltage pairs in the I-V curves is not constant.

## 4 Characterization Data for PV Model Inputs

After the field deployments were completed, measurements were performed to provide data suitable for use in deriving inputs for models for estimating the performance of PV modules. NREL performed indoor measurements at STC and low irradiance conditions (200 W/m<sup>2</sup>). The CFV Solar Test Laboratory measured the irradiance-temperature characteristics per IEC 61853 [1] and the temperature coefficients per IEC 61646 [3] or IEC 61215 [2]. Sandia measured coefficients and parameters for use with the Sandia PV array performance model. These data are provided in the file CharacterDataForPVModels.xlsx, which is distributed with the files listed in Table 3-1. Also included in the file are other PV module-specific information and their deployment histories.

## 5 Performance Changes from Deployments

The characterization data described in Section 4 depict the performance of the PV modules at the end of their deployments rather than prior to their deployments. This better accommodated the field deployment schedule and spared some expense and time because PV modules that failed or were damaged did not undergo the characterization tests nor are data for failed or damaged PV modules included in any of the I-V curve data sets. During the time of the deployments, we were also fortunate that the test laboratories upgraded their equipment and capabilities, which provided better characterization results.

To provide information on degradation in performance from the deployments, we compared the average performance for irradiances near 1,000 W/m<sup>2</sup> at the beginning and end of each deployment. Deployments were for approximately 13 months, so calendar days common to both the beginning and end were used to minimize the effects of seasonal changes in spectral and angle-of-incidence effects. Deployments at Cocoa were from January 22, 2011, to March 4, 2012; consequently, we compared performances at the start from January 22, 2011, to March 4, 2011, with performances at the end from January 22, 2012, to March 4, 2012. Similarly, for the Golden deployments, we compared performances from August 14, 2012, to September 24, 2012, with performances from August 14, 2013, to September 24, 2013. The ending deployment months for Eugene were cloudy and provided few data points; consequently, we compared performances from December 20, 2012, to January 30, 2013, with performances from November 10, 2013, to November 23, 2013. In addition, the irradiance screening criteria were relaxed for Eugene to provide a minimum of 20 data points for each start and end period.

I-V curve data for the data analysis were screened for:

- POA irradiance measured with CMP 22 pyranometer from 975 W/m<sup>2</sup> to 1,025 W/m<sup>2</sup> (950 W/m<sup>2</sup> to 1,050 W/m<sup>2</sup> for Eugene)
- Change in POA irradiance during I-V curve measurement of less than 2 W/m<sup>2</sup>, measured with both the CMP 22 and LI-COR pyranometers.

PV module  $I_{sc}$  and  $P_m$  values from the I-V curves were corrected to a rating condition of 1,000 W/m<sup>2</sup> irradiance and 25°C cell temperature using Eqns. 3 and 4.

$$I_{scR} = [ 1000 / E_{poa} ] \cdot [ I_{sc} / S_d ] \div [ 1 + \alpha \cdot (T_c - 25) ] \quad (3)$$

$$P_{mR} = [ 1000 / E_{poa} ] \cdot [ P_m / S_d ] \div [ 1 + \gamma \cdot (T_c - 25) ] \quad (4)$$

where:

- $E_{poa}$  = POA irradiance, W/m<sup>2</sup>
- $\alpha$  =  $I_{sc}$  correction factor for temperature, °C<sup>-1</sup>
- $T_c$  = PV cell temperature, PV module back-surface temperature plus 2°C per 1,000 W/m<sup>2</sup> irradiance
- $S_d$  = PV module soiling derate (field 38 from Table 3-3)
- $\gamma$  =  $P_m$  correction factor for temperature, °C<sup>-1</sup>

$P_m$  ratings were also determined using the self-irradiance principle where the ratio of  $I_{sc}$  at STC to the temperature-corrected  $I_{sc}$  replaces the first term of Eqn. 4. After simplifying, this relationship is shown as Eqn. 5.

$$P_{mRs} = [ P_m \cdot I_{sc0} / I_{sc} ] \cdot [ 1 + \alpha \cdot (T_c - 25) ] \div [ 1 + \gamma \cdot (T_c - 25) ] \quad (5)$$

where:

$I_{sc0}$  = short-circuit current at STC, A

Using Eqn. 5 to compare performance between start and end periods identifies changes in PV cell performance, usually fill-factor for small changes, because the effects on performance due to soiling, spectrum, angle-of-incidence, and degradation of the PV module cover and encapsulation are avoided. Performance changes using Eqn. 3 may indicate different spectral irradiance conditions or degradation of the PV module cover and encapsulation, which reduce the light received by the PV cell and the current produced. Other factors to consider when comparing ratings are potential degradation of the pyranometer sensor and errors in values of the temperature coefficients.

Table 5-1 provides the calculated changes in performance ratings for each of the PV module deployments. PV modules are grouped by manufacturer and model. Because the same PV modules were deployed at the Cocoa and Eugene sites and the characterization measurements in Section 4 were measured after the Eugene deployments, the changes in performance at the Eugene site should be added to those at the Cocoa site to determine Cocoa performance relative to the characterization data.

Assuming no changes in performance between deployments, the end ratings for Cocoa should equal the start ratings for Eugene. This was mostly true for the crystalline silicon and CIGS PV modules, but less so for the CdTe and a-Si modules, which are more sensitive to variations in solar spectrum. For these PV modules, the spectral conditions for Eugene in the early winter, when that deployment began, are less favorable than the late winter and early spring conditions for the deployment that ended in Cocoa. Site decreases in performance for the a-Si PV modules may be related to their deployment histories. When a-Si PV modules are deployed to a cooler site, the performance stabilizes over time to a lower efficiency, and with seasonal oscillations [6]. Deployment histories are provided in the file CharacterDataForPVModels.xlsx, which is distributed with the files listed in Table 3-1.

Because of uncertainties in deriving the ratings in Table 5-1, relative changes of less than 0.5% do not need to be considered when using the data for PV module model validations. If the PV modules can be assumed to be linear devices [7], modelers can determine the irradiance using the measured  $I_{sc}$  and the self-irradiance principle if the models to be validated only account for variations in irradiance and PV module temperature (not spectrum or angle-of-incidence effects). Performance changes during the deployments would then be represented by the  $P_{mRs}$  values in Table 5-1, which are usually less.

Because the PV modules in Table 5-1 are limited in number and the deployments were of a relatively short duration, their performance changes should not be considered representative of a

PV module's technology. In addition, users are encouraged to perform their own analysis of performance changes using other techniques as appropriate.

**Table 5-1. PV Module Changes in Derived Performance Ratings from Start to End of Deployments**

PV Module	Site	$I_{scR}$			$P_{mR}$			$P_{mRs}$
		Start (A)	End (A)	Change (%)	Start (W)	End (W)	Change (%)	Change (%)
xSi12922	Cocoa	4.977	4.986	0.2	79.82	79.87	0.1	0.3
	Eugene	5.047	4.979	-1.3	81.84	81.07	-0.9	0.4
xSi11246	Golden	4.913	4.930	0.4	76.62	76.24	-0.5	-1.0
mSi460A8	Cocoa	4.936	4.949	0.3	79.34	79.58	0.3	0.4
	Eugene	4.962	4.898	-1.3	80.06	79.13	-1.2	0.1
mSi460BB	Golden	4.913	4.935	0.5	79.41	79.73	0.4	-0.2
mSi0166	Cocoa	2.684	2.679	-0.2	45.51	45.45	-0.1	0.0
	Eugene	2.709	2.678	-1.1	45.71	45.04	-1.5	-0.4
mSi0188	Cocoa	2.682	2.683	0.0	45.21	45.24	0.1	0.4
	Eugene	2.709	2.678	-1.2	45.45	44.63	-1.8	-0.5
mSi0247	Golden	2.660	2.668	0.3	45.48	45.63	0.3	0.0
mSi0251	Golden	2.663	2.672	0.3	44.79	44.98	0.4	-0.2
CdTe75638	Cocoa	1.175	1.186	0.9	67.10	66.86	-0.4	-0.9
	Eugene	1.156	1.131	-2.1	63.11	62.79	-0.5	-0.8
CdTe75669	Golden	1.150	1.169	1.6	64.56	64.77	0.3	-1.5
CIGS39017	Cocoa	6.474	6.330	-2.2	156.43	150.63	-3.7	-1.0
	Eugene	6.387	6.217	-2.7	150.46	147.47	-2.0	0.7
CIGS39013	Golden	6.109	5.961	-2.4	141.93	135.33	-4.7	-2.5
CIGS8-001	Cocoa	2.488	2.522	1.4	79.38	69.59	-12.3	-13.1
	Eugene	2.523	2.501	-0.8	69.07	67.64	-2.1	-2.2
CIGS1-001	Golden	2.488	2.501	0.5	76.34	75.18	-1.5	-2.2
HIT05667	Cocoa	5.434	5.416	-0.3	216.33	212.71	-1.7	-1.0
	Eugene	5.462	5.367	-1.8	215.22	210.56	-2.2	-0.4
HIT05662	Golden	5.470	5.474	0.1	215.55	214.26	-0.6	-0.9
aSiMicro03036	Cocoa	0.823	0.829	0.7	112.17	110.31	-1.7	-1.9
	Eugene	0.744	0.747	0.3	101.17	97.10	-4.0	-4.4
aSiMicro03038	Golden	0.802	0.814	1.5	107.26	108.29	1.0	-0.8
aSiTandem72-46	Cocoa	1.082	1.091	0.9	39.69	39.56	-0.3	-0.8
	Eugene	1.034	1.031	-0.3	36.35	35.53	-2.3	-2.0
aSiTandem90-31	Golden	1.111	1.127	1.4	40.79	41.30	1.3	-0.4
aSiTriple28324	Cocoa	4.683	4.709	0.5	69.39	64.81	-6.6	-6.7
	Eugene	4.205	4.155	-1.2	59.65	56.43	-5.4	-4.3
aSiTriple28325	Golden	4.519	4.626	2.4	62.21	63.09	1.4	-1.0

## References

1. International Electrotechnical Commission (IEC) 61853-1. “Photovoltaic (PV) Module Performance Testing and Energy Rating – Part 1: Irradiance and Temperature Performance Measurements and Power Rating.” Geneva: IEC Central Office, 2011.
2. IEC 61215. “Crystalline Silicon Terrestrial Photovoltaic (PV) Modules – Design Qualification and Type Approval.” Geneva: IEC Central Office, 2005.
3. IEC 61646. “Thin-film Terrestrial Photovoltaic (PV) Modules – Design Qualification and Type Approval.” Geneva: IEC Central Office, 2008.
4. King, D.L.; Boyson, W.E.; Kratochvill, J.A. *Photovoltaic Array Performance Model*. SAND-2004-3535. Albuquerque, NM: Sandia National Laboratories, 2004.
5. International Organization for Standardization (ISO)/IEC 17025. “General Requirements for The Competence of Testing and Calibration Laboratories.” Geneva: IEC Central Office, 2005.
6. Rütther, R.; Montenegro, A.A.; del Cueto, J.; Rummel, S.; Anderberg, A.; Von Roedern, B.; Tamizh-Mani, G. “Performance Test of Amorphous Silicon Modules in Different Climates — Year Four: Progress in Understanding Exposure History Stabilization Effects.” Presented at the 33rd IEEE Photovoltaic Specialists Conference, San Diego, California. May 11–16, 2008.
7. IEC 60904-10. “Photovoltaic Devices – Part 10: Methods of Linearity Measurement.” Geneva: IEC Central Office, 2009.

## Appendix A – Quality Assessment Methods

QA methods were implemented to exclude data not meeting quality thresholds from being included in data distributed outside of NREL. The QA methods are based on those previously established to provide ISO 17025 [1] accredited data for PV modules installed on the PERT at NREL.

The QA methods consist of daily checks and calculations of daily statistics and metrics to ensure that measurements are performed as expected. They detect trends and data outside established limits.

### A.1 I-V Curve Data

Software written to interface with the Daystar MT5 multi-tracer and the NREL database performs a number of checks to ensure proper operation of the MT5 multi-tracer and data processing:

- Checks the number of I-V curves measured for each PV module during daytime hours. I-V curves are needed between sunrise and sunset (including the effects of mountains for Golden). I-V curves are measured at 15-minute intervals (Golden) or 5-minute intervals (Cocoa and Eugene). The number of I-V curve XML files provided by the MT5 multi-tracer is compared to that expected during daytime hours. Discrepancies are investigated by the engineer or database support, and corrective action is taken as appropriate.
- Checks the number of I-V curves measured for each PV module for irradiance conditions equal to or greater than  $50 \text{ W/m}^2$  (Golden) or  $20 \text{ W/m}^2$  (Cocoa and Eugene). If less than this lower limit, the analysis software excludes the data. Compares the number of I-V curves measured with the irradiance equal to or greater than the lower limit with the number of daytime XML files.
- Checks the number of I-V curves measured for each PV module under stable irradiance conditions. The irradiances measured with the POA CMP 22 and LI-COR pyranometers immediately before and after the I-V curve measurement indicate the stability of the irradiance during the I-V curve measurements. (If any of the before-after differences are more than  $5 \text{ W/m}^2$ , the analysis software excludes the data.) Compares the number of I-V curves measured under stable irradiance conditions to the number of I-V curves measured with the irradiance greater than or equal to the lower limit.
- Checks the number of I-V curves measured for each PV module that had its I-V curve parameters successfully determined using the test methods from ASTM Standard E 1036-08 [2] and that met NREL data-fitting criteria: the slope of the curve at  $I_{sc}$  is negative; the difference between the values of  $I_{sc}$ ,  $P_{mp}$ , and  $V_{oc}$  determined using the test methods from ASTM E 1036-08 [2] and the values provided by the MT5 multi-tracer are less than or equal to 1%; and the  $I_{sc}$  plus the product of  $V_{mp}$  and the slope at  $I_{sc}$  is less than  $I_{mp}$ . (If unsuccessful, the analysis software excludes the data.) Compares the number of I-V curves with the successful application of the test methods of ASTM E 1036-08 and meeting the NREL data-fitting criteria to the number of I-V curves measured under stable irradiance and for irradiance equal to or greater than the lower limit.

Software is checked each day for unauthorized changes or corruptions by use of the 512-bit version of the secure hash algorithm (SHA-512), developed by the United States National Security Agency and published by the National Institute of Standards and Technology, to check for application code integrity. The algorithm generates a 512-bit hash value, represented by a 128-digit hexadecimal number that is unique to each application version. A change of a single bit within the software version generates a different SHA-512 hexadecimal value, which indicates a change in the software.

## **A.2 Meteorological and Other Data**

For the meteorological and other data in the daytime XML files that are transferred to the database, data checks are performed by comparing redundant measurements to each other, by comparing similar measurements to each other, by minimum and maximum limits, and by metrics that show consistency between dependent parameters. These data checks are made using the data measurement immediately before the I-V curve measurement. Limits define expectations of possible data values.

### **A.2.1 POA Irradiance with CMP 22 and LI-COR Pyranometers**

- Maximum Irradiance – Determine the daily maximum irradiance for the CMP 22 and LI-COR. Passing criterion: less than  $1,500 \text{ W/m}^2$ .
- Minimum Irradiance – Determine the daily minimum irradiance for the CMP 22 and LI-COR. Passing criterion: greater than  $-5 \text{ W/m}^2$ .
- Daily Total Irradiance – Compare the daily totals for the CMP 22 and LI-COR. Passing criteria: within 5% and  $0.40 \text{ kWh/m}^2/\text{day}$ .

### **A.2.2 PV Module Back-Surface Temperature**

- Initial – Determine the PV module back-surface temperature for the first daytime XML file of the day (i.e., within 15 minute of sunrise [Golden] or within 5 minutes of sunrise [Cocoa and Eugene] and which will have minimal solar heating). Passing criterion: PV module back-surface temperature within  $3^\circ\text{C}$  of the average PV module back-surface temperature for all PV modules for their first XML file of the day.
- Minimum – Determine the minimum PV module back-surface temperature for the day. Passing criterion: greater than  $-34^\circ\text{C}$ .
- Maximum – Determine the maximum PV module back-surface temperature for the day. Passing criteria: within  $12^\circ\text{C}$  of the average maximum PV module back surface temperature for all PV modules and less than  $75^\circ\text{C}$ .

### **A.2.3 PV Module Performance Ratio**

- Irradiance and PV Module I-V Curve Relationship – Calculate the daily performance ratio (PR) using  $P_m$  from the I-V curves and the CMP 22 POA irradiance measurements, and the PV module power rating at STC. Use data for I-V curves that met the successful application of the ASTM E 1036-08 test methods [2] and the NREL I-V curve data fitting criteria. Passing criterion:  $0.3 < \text{PR} < 1.1$  (Cocoa and Eugene) or  $0.6 < \text{PR} < 1.1$  (Golden).

$$PR = \frac{\sum P_m}{P_{stc} \times \sum E_{POA} \div 1000}$$

#### **A.2.4 Enclosure Air Temperature for MT5 Multi-tracer**

- Maximum – Determine the daily maximum temperature. Passing criterion: less than 35°C (Cocoa and Eugene) or less than 30°C (Golden).
- Minimum – Determine the daily minimum temperature. Passing criterion: greater than 15°C (Cocoa and Eugene) or greater than 20°C (Golden).

#### **A.2.5 Dry Bulb Temperature**

- Maximum – Determine the daily maximum temperature. Passing criterion: less than 45°C.
- Minimum – Determine the daily minimum temperature. Passing criterion: greater than -34°C.

#### **A.2.6 Relative Humidity**

- Maximum – Determine the daily maximum humidity. Passing criterion: less than 101%.
- Minimum – Determine the daily minimum humidity. Passing criterion: greater than 0%.

#### **A.2.7 Atmospheric Pressure**

- Maximum – Determine the daily maximum atmospheric pressure. Passing criterion: less than 1,086 mb (Cocoa and Eugene) or 905 mb (Golden).
- Minimum – Determine the daily minimum barometric pressure. Passing criterion: greater than 870 mb (Cocoa and Eugene) or 724 mb (Golden).

#### **A.2.8 Global Horizontal Irradiance**

- Maximum Irradiance – Determine the daily maximum irradiance. Passing criterion: less than 1,500 W/m<sup>2</sup>.
- Minimum Irradiance – Determine the daily minimum irradiance. Passing criterion: greater than -5 W/m<sup>2</sup>.

#### **A.2.9 Diffuse Horizontal Irradiance**

- Maximum Irradiance – Determine the daily maximum irradiance. Passing criterion: less than 1,500 W/m<sup>2</sup>.
- Minimum Irradiance – Determine the daily minimum irradiance. Passing criterion: greater than -5 W/m<sup>2</sup>.

#### **A.2.10 Direct Normal Irradiance**

- Maximum Irradiance – Determine the daily maximum irradiance. Passing criterion: less than 1,500 W/m<sup>2</sup>.
- Minimum Irradiance – Determine the daily minimum irradiance. Passing criterion: greater than -5 W/m<sup>2</sup>.

### **A.2.11 Global Horizontal Daily Total Irradiance**

- Compare the measured global horizontal daily total irradiance with the daily total irradiance calculated as the sum of the measured diffuse horizontal irradiance plus the direct normal irradiance component for a horizontal surface. Passing criterion: within 3%.

## **A.3 Data Exclusion Rules**

The rules followed for excluding suspect data differed slightly because of slight differences in the equipment used for the Cocoa/Eugene data collection and that used for the Golden data. The equipment for the Cocoa/Eugene data collection was specifically procured for that work whereas the Golden data collection effort used equipment already in place at NREL. Both sets of equipment used Daystar MT5 multi-tracers and Campbell Scientific data loggers for acquisition of sensor signals. For both sets of equipment, the Daystar multi-tracers measured the PV module I-V curves, the POA irradiances, the PV module temperatures, and the enclosure air temperature for the Daystar multi-tracer. The other meteorological data were measured by the Campbell Scientific data loggers, except for the Golden data where the dry bulb temperature was measured using the Daystar multi-tracer.

The following rules were used to exclude data judged to be potentially erroneous:

- All data for the day are excluded if the criteria fail for POA irradiance (A.2.1), enclosure air temperature for MT5 multi-tracer (A.2.4), or dry bulb temperature (A.2.5, Golden data only).
- All data for the day are excluded for an individual PV module if the criterion fails for its PV module back surface temperature (A.2.2) or its PV module performance ratio (A.2.3).
- All data measured by the Campbell Scientific data logger for the day are excluded if the criteria fail for dry bulb temperature (A.2.5, Cocoa and Eugene data only), relative humidity (A.2.6), atmospheric pressure (A.2.7), global horizontal irradiance (A.2.8), diffuse horizontal irradiance (A.2.9), direct normal irradiance (A.2.10), or global horizontal daily total irradiance (A.2.11). These excluded data are shown in the data files as missing data with values of -9999.
- All data for the day are excluded if snow or ice is present on the PV modules or other adverse situations exist as determined by the engineer.

## **A.4 References**

1. ISO/IEC 17025. "General requirements for the competence of testing and calibration laboratories." Geneva: IEC Central Office, 2005.
2. ASTM International. "Standard Test Methods for Electrical Performance of Nonconcentrator Terrestrial Photovoltaic Modules and Arrays Using Reference Cells." ASTM Standard E1036-08. West Conshohocken, PA: ASTM International. 2008.

## Appendix B – Measurement Uncertainty Analysis

This uncertainty analysis is based on an uncertainty analysis previously developed for the PERT system in Golden and is extended to include the mobile PERT system (mPERT) deployed in Cocoa and Eugene. The mPERT system includes additional meteorological measurements collected by a Campbell Scientific CR1000 logger. The additional meteorological measurements include irradiance (direct normal, diffuse horizontal, and global horizontal) and ambient weather conditions (dry bulb temperature, barometric pressure, relative humidity, and precipitation).

### B.1 Reference to Norms and Standards

- ASTM E1036: “Standard Test Methods for Electrical Performance of Nonconcentrator Terrestrial Photovoltaic Modules and Arrays Using Reference Cells” [1]
- Procedure ISO GUM: “International Organization for Standardization, Guide to the Expression of Uncertainty in Measurement.” Geneva: ISO, 1995, ISBN 92-67-10188-9 [2]

### B.2 Overview

This uncertainty analysis is for measurements of I-V characteristics of solar PV panels deployed outdoors under natural illumination. Rather than expressing performance as translated to a standard operating condition (e.g., 25°C and 1,000 W/m<sup>2</sup>), raw performance data are reported along with prevailing meteorological conditions, which include irradiance (POA, direct normal, diffuse horizontal, and global horizontal), module temperature ( $T_{\text{mod}}$ ), dry bulb temperature, barometric pressure, relative humidity, and precipitation. The uncertainty analysis is conducted for the PV panels’ I-V characteristics along with uncertainty for the prevailing meteorological conditions.

### B.3 Procedure

Table B-1 summarizes the standard uncertainty components, including the calculated value of uncertainty for a reference case and the statistical coverage factor. All uncertainty components are given in percentage of the value with a 1.25-m<sup>2</sup> module as the reference case, as described in Figure B-1. Uncertainty of temperature is reported in degrees C. This analysis is provided as an example of how uncertainty is calculated for every I-V measurement conducted by the PERT and mPERT experiment. All uncertainties are based upon a 1-year calibration interval.

**Table B-1. Summary of Standard Uncertainty Components**

<b>Uncertainty Component</b>	<b>Source of Uncertainty</b>	<b>Value of Uncertainty (%)<sup>a</sup></b>	<b>Coverage Factor</b>
<b>U<sub>Voc</sub></b>	<b>Uncertainty in test device V<sub>oc</sub></b>	<b>0.260</b>	<b>2</b>
U <sub>V-DMM</sub>	Measured test device voltage using MT5	0.225	Rectangular
S <sub>VocFit</sub>	Standard deviation of intercept for linear fit near V <sub>oc</sub>	0.006	N <sub>Voc</sub>
δ	Smallest resolvable digit	0.005	Sqrt(12)
U <sub>V-Cal</sub>	Uncertainty of the voltage standard used to calibrate the curve tracer	0.012	Rectangular
<b>U<sub>Isc</sub></b>	<b>Uncertainty in test device I<sub>sc</sub></b>	<b>0.277</b>	<b>2</b>
U <sub>I-DMM</sub>	Measured test device current using MT5	0.231	Rectangular
S <sub>IscFit</sub>	Standard deviation of intercept for linear fit near I <sub>sc</sub>	0.006	N <sub>Isc</sub>
δ	Smallest resolvable digit.	0.006	Sqrt(12)
U <sub>I-Cal</sub>	Uncertainty of the current standard used to calibrate the curve tracer	0.064	Rectangular
<b>U<sub>Pmax</sub></b>	<b>Uncertainty in test device P<sub>max</sub></b>	<b>0.409</b>	<b>2</b>
U <sub>V-DMM</sub>	Measured test device voltage using MT5	0.247	Rectangular
U <sub>I-DMM</sub>	Measured test device current using MT5	0.239	Rectangular
U <sub>P-fit</sub>	Error in P <sub>max</sub> from the polynomial fit	0.060	Gaussian
U <sub>V-Cal</sub>	Uncertainty in MT5 voltage calibration	0.012	Rectangular
U <sub>I-Cal</sub>	Uncertainty in MT5 current calibration	0.064	Rectangular
<b>U<sub>Imax</sub></b>	<b>Uncertainty in test device I<sub>mp</sub></b>	<b>0.343</b>	<b>2</b>
<b>U<sub>Vmax</sub></b>	<b>Uncertainty in test device V<sub>mp</sub></b>	<b>0.334</b>	<b>2</b>
<b>U<sub>FF</sub></b>	<b>Uncertainty in test device fill factor</b>	<b>0.558</b>	<b>2</b>

<b>Uncertainty Component</b>	<b>Source of Uncertainty</b>	<b>Value of Uncertainty (%)<sup>a</sup></b>	<b>Coverage Factor</b>
<b>U<sub>Tmod</sub></b>	<b>Uncertainty in back-of-module temperature</b>	<b>1.92°C</b>	<b>2</b>
U <sub>T-Mount</sub>	Thermocouple mounting and wiring method	0.5°C	Rectangular
U <sub>T-DMM</sub>	Uncertainty in MT5 temperature measurement	1.5°C	Rectangular
U <sub>TC</sub>	Uncertainty in thermocouple device	0.5°C	Rectangular
<b>U<sub>Irr</sub></b>	<b>Uncertainty in POA irradiance -0 to 60 degrees</b>	<b>2.416</b>	<b>2</b>
U <sub>Irr-DMM</sub>	Uncertainty in MT5 Aux channel	0.971	Rectangular
U <sub>Irr-Cal</sub>	Pyranometer device calibration uncertainty	1.750	2
U <sub>Irr-Angle</sub>	Uncertainty in mounting angle	0.508	Rectangular
U <sub>Irr-Tcoef</sub>	Uncertainty from pyranometer temperature coefficient	0.5	Rectangular
U <sub>Irr-Lin</sub>	Uncertainty from pyranometer nonlinearity from 50 –1,500 W/m <sup>2</sup>	0.30	Rectangular
U <sub>Irr-Stab</sub>	Pyranometer stability per year	0.50	Rectangular
U <sub>Irr-TypeA</sub>	Far-infrared response, “Type A” offset	0.54	Rectangular
<b>UIrr 60-80</b>	<b>Uncertainty in POA irradiance - 60 to 80 degrees</b>	<b>9.82</b>	<b>2</b>
<b>U<sub>DNI</sub></b>	<b>Uncertainty in direct normal irradiance</b>	<b>1.36</b>	<b>2</b>
<b>U<sub>DHI</sub></b>	<b>Uncertainty in diffuse horizontal irradiance</b>	<b>2.56</b>	<b>2</b>
<b>U<sub>GHI</sub></b>	<b>Uncertainty in global horizontal irradiance</b>	<b>2.14</b>	<b>2</b>
<b>U<sub>Tamb</sub></b>	<b>Uncertainty in outdoor ambient temperature</b>	<b>0.38°C</b>	<b>2</b>
<b>U<sub>RH</sub></b>	<b>Uncertainty in relative humidity</b>	<b>3.46%RH</b>	<b>2</b>
<b>U<sub>Press</sub></b>	<b>Uncertainty in barometric pressure</b>	<b>0.11</b>	<b>2</b>
<b>UPrecip</b>	<b>Uncertainty in precipitation</b>	<b>5.77</b>	<b>2</b>

<sup>a</sup> Unless otherwise indicated.

## B.4 Assumptions Made for Uncertainty Analysis

Unless stated otherwise, uncertainty is determined using standard uncertainty analysis based upon [2, 3, 4] and stated as a percentage of value. The analysis is based upon the best measurement capability and represents the smallest uncertainty of nearly ideal photovoltaic reference devices. This means that the devices should be stable with no measurable short-term degradation or light sensitivity.

To properly express the uncertainty as a percentage, a typical I-V case is used so the proper measurement ranges and resolutions can be converted to a percentage. The I-V curve for a typical large-area PV module of the type that would be tested on the PERT test bed is shown in Figure B-1. All further uncertainty analysis in this document is based on this PV module.

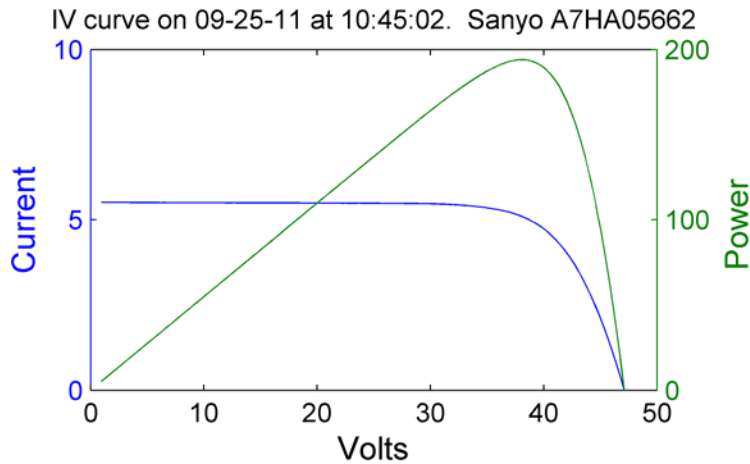


**Figure B-1. I-V curve for representative PV module**

Parameters at 1,000 W/m<sup>2</sup> plane-of-array irradiance and 56.7°C module temperature:  $I_{sc}$  5.51 A;  $V_{oc}$  47.1 V;  $I_{mp}$  5.11 A;  $V_{mp}$  37.96 V. Aperture area: 1.204 m<sup>2</sup>. Total area: 1.256 m<sup>2</sup>. Indoor ambient temperature: 24.5°C.

## B.5 Uncertainty in $V_{oc}$

The standard uncertainty in measurement of  $V_{oc}$ -  $U_{V_{oc}}$  is largely based on the elemental uncertainty of the data acquisition equipment  $u_{V-DMM}$ , along with uncertainty in the linear fit near  $V_{oc}$ :  $s_{V_{oc}Fit}$ . An equation for  $U_{V_{oc}}$  is shown in Eqn. (1).

$$U_{V_{oc}} = 2 \left[ \left( \frac{u_{V-DMM}}{\sqrt{3}} \right)^2 + \left( \frac{s_{V_{oc}Fit}}{N_{V_{oc}}} \right)^2 + \left( \frac{\delta}{\sqrt{12}} \right)^2 + \left( \frac{u_{V-Cal}}{\sqrt{3}} \right)^2 \right]^{0.5} \quad (1)$$

Note that resistive voltage loss between the MT5 load and the solar module is not included in Eqn. 1 because voltage is monitored on a four-wire Kelvin probe and will therefore not be subject to resistive voltage loss. The calculation of  $u_{V-DMM}$  requires knowledge of the voltage range and uncertainty for this measurement on the MT5 multi-tracer.

$$u_{V-DMM} = ([\%reading + temperature correction] + [\%range + temp. correction]) \quad (2)$$

In the case of the MT5 multi-tracer, the percent reading and percent range accuracies are 0.1% and 0.02%, respectively. The temperature correction for the ambient temperature of the data acquisition unit is 0.005 %/°C. The MT5 multi-tracer is in an indoor climate-controlled room with an expected temperature window of 25°C ± 5°C (plus an uncertainty in indoor ambient temperature of 1.76°C). The indoor ambient temperature is referred to elsewhere as the air temperature within the cabinet containing the MT5 multi-tracer. Therefore, the value for  $u_{V-DMM}$  given a 30°C indoor ambient temperature, 47.4 V measurement, and 80 V range is:

$$u_{V-DMM} = 100 * \{[(0.1+(31.76-25)*0.005)*0.01*47.4]+[(0.02+(31.76-25)*0.005)*0.01*80]\}/47.4$$

$$u_{V-DMM} = 0.22\%$$

The next component of uncertainty in the calculation of  $V_{oc}$  is the uncertainty of the linear fit near  $V_{oc}$ . A linear fit through the I-V data points near  $V_{oc}$  is conducted given the following constraints: at least five (I,V) points exist where  $V > 0.9 * V_{oc}$  and  $I < 0.2 * I_{sc}$ .

The uncertainty in the  $V_{oc}$  linear fit is expressed as  $(s_{V_{oc}Fit} / N_{V_{oc}})^2$ , where  $s_{V_{oc}Fit}$  is the standard error of the linear fit's X-intercept in the linear region of interest, and  $N_{V_{oc}}$  is the number of data points in the fit [5]. For the example I-V curve here, the values of  $s_{V_{oc}Fit}$  and  $N_{V_{oc}}$  are 0.0062 % and 9, respectively.

Alternately, ASTM E1036 Section 8.6.1 [1] allows a measured I-V data pair to be used directly for the measured  $V_{oc}$ , if  $I$  is  $0.0 \pm 0.001 I_{sc}$ . In this case,  $V_{oc}$  is directly measured, and  $s_{V_{oc}Fit} = 0$ .

The third component of uncertainty in the calculation of  $U_{V_{oc}}$  is the uncertainty due to the 15-bit resolution of the MT5 curve tracer. This value is based on  $\delta$ , the smallest resolvable digit, and carries a coverage value of  $\sqrt{12}$  [6]. Expressed as a percentage of reading, this value is  $(0.00244 \text{ V} / 47.4 \text{ V}) = 0.005\%$ .

The fourth component of uncertainty in  $U_{V_{oc}}$  is  $u_{V-Cal}$ , the uncertainty of the voltage standard used to calibrate the curve tracer. Assuming a Wavetek 9100 calibrator is used as the voltage standard, the manufacturer stated that uncertainty on the 80-V channel is 0.0065% + 4.48 mV. Based as a percentage of the output voltage during calibration (80 V), the uncertainty  $u_{V-Cal}$  is:

$$u_{V-Cal} = (0.000065 * 80 + 0.00448)/80 * 100 = 0.012 \%$$

Given these values and the coverage factors provided in Table B-1,

$$U_{V_{oc}} = 2 \left[ \left( \frac{0.22}{\sqrt{3}} \right)^2 + \left( \frac{0.006}{9} \right)^2 + \left( \frac{0.005}{\sqrt{12}} \right)^2 + \left( \frac{0.012}{\sqrt{3}} \right)^2 \right]^{0.5}$$

$$= 0.26\%$$

## B.6 Uncertainty in $I_{sc}$

A similar analysis is conducted for  $I_{sc}$ . The equation for expanded uncertainty  $U_{I_{sc}}$  is shown in Eqn. (3):

$$U_{Isc} = 2 \left[ \left( \frac{u_{I-DMM}}{\sqrt{3}} \right)^2 + \left( \frac{s_{IscFit}}{N_{Isc}} \right)^2 + \left( \frac{\delta}{\sqrt{12}} \right)^2 + \left( \frac{u_{I-Cal}}{\sqrt{3}} \right)^2 \right]^{0.5} \quad (3)$$

The calculation for  $u_{I-DMM}$  is dependent on the current measurement accuracy of the MT5 curve tracer:

$$u_{I-DMM} = ([\%reading + temperature\ correction] + [\%range + temp.\ correction]) \quad (4)$$

As was the case with voltage measurements, for current measurements with the MT5, the % reading and % range accuracies are 0.1% and 0.02%, respectively. The indoor ambient temperature correction is also 0.005 %/°C. Therefore, the value for  $u_{I-DMM}$  given a 30°C indoor ambient temperature, 5.51A  $I_{sc}$  measurement and 10-A range is:

$$u_{I-DMM} = 100 * \{[(0.1 + (31.76-25)*0.005)*0.01*5.51] + [(0.02+(31.76-25)*0.005)*0.01*10]\} / 5.51$$

$$u_{I-DMM} = 0.23\%$$

The component of uncertainty associated with the linear fit near  $I_{sc}$  is again expressed as  $(s_{IscFit} / N_{Isc})^2$ , where  $s_{IscFit}$  is the standard error of the linear fit's Y-intercept in the linear region of interest, and  $N_{Isc}$  is the number of data points in the fit. For the linear fit near  $I_{sc}$ , (I,V) points are chosen where  $I > 0.96 * I_{sc}$  and  $V < 0.2 * V_{oc}$ . Five points must exist in this region to conduct the linear fit.

For the example I-V curve given in Figure B-1, the values of  $s_{IscFit}$  and  $N_{Isc}$  are 0.00035 A and 34, respectively. Expressed as a percentage of reading, this value is  $s_{IscFit} = (0.00035 \text{ A} / 5.51 \text{ A}) * 100 = 0.0064\%$ .

Alternately, ASTM E1036 Section 8.5.1 allows a measured I-V data pair to be used directly for the measured  $I_{sc}$ , if  $V$  is  $0.0 \pm 0.005 V_{oc}$  [1]. In this case,  $I_{sc}$  is directly measured, and  $s_{IscFit} = 0$ .

For the bit resolution error of the MT5 measurement, a similar calculation is required to above.  $\delta$ , the smallest resolvable digit, is calculated by

$$\delta = (10 / 2^{15}) / 5.51 * 100 = 0.0055\%.$$

The final elemental uncertainty is the uncertainty of the calibration source used to calibrate current. Again, assuming a Wavetek 9100 calibrator as a current calibration source, the manufacturer supplied uncertainty on a 10-A channel is 0.055% + 0.94 mA. Based as a percentage of the output current during calibration (10 V), the uncertainty  $u_{I-Cal}$  is:

$$u_{I-Cal} = (0.00055 * 10 + 0.00094) / 10 * 100 = 0.064 \%$$

Given these values and the coverage factors provided in Table B-1,

$$U_{Isc} = 2 \left[ \left( \frac{0.23}{\sqrt{3}} \right)^2 + \left( \frac{0.0064}{34} \right)^2 + \left( \frac{0.0055}{\sqrt{12}} \right)^2 + \left( \frac{0.064}{\sqrt{3}} \right)^2 \right]^{0.5}$$

$$= 0.28\%.$$

## B.7 Uncertainty in $P_{max}$ , $V_{max}$ , $I_{max}$ and Fill Factor

The maximum power,  $P_{max}$ , is defined as the maximum of the product of the current and voltage of the panel. The current at  $P_{max}$ , is defined as  $I_{max}$  while the voltage at  $P_{max}$  is  $V_{max}$ . The largest measured power may not be the maximum power because of noise on the measured current versus voltage. For this reason, the maximum power is obtained by a polynomial curve fit to a restricted set of data points. The  $(P, V)$  data points chosen for this polynomial fit must meet the requirements  $V > 0.8 * V_{max}$  and  $P > 0.85 P_{max}$ . If at least seven  $(P, V)$  data points exist in this region, a fourth-order polynomial fit is applied. A first derivative of the fitted equation provides the location of  $P_{max}$  and  $V_{max}$  based on the polynomial fit, by locating the real root closest to  $V_{max}$ .

The uncertainty  $U_{P_{max}}$  contains several elements previously discussed in the preceding sections on  $V_{oc}$  and  $I_{sc}$ . A full equation is given in Eqn. (5):

$$U_{P_{max}} = 2 \left[ \left( \frac{u_{I-DMM}}{\sqrt{3}} \right)^2 + \left( \frac{u_{V-DMM}}{\sqrt{3}} \right)^2 + \left( \frac{u_{P-fit}}{2} \right)^2 + \left( \frac{u_{I-Cal}}{\sqrt{3}} \right)^2 + \left( \frac{u_{V-Cal}}{\sqrt{3}} \right)^2 \right]^{0.5} \quad (5)$$

The uncertainty  $u_{P,fit}$  shown in the above equation refers to the uncertainty arising from the polynomial fit near  $P_{max}$ . This error was determined to be less than 0.06% in a prior publication detailing a computer-based Monte Carlo analysis [7]. Indeed, for the example considered here, the standard deviation in the  $P_{max}$  fit using a 47-point, fifth-degree polynomial was 0.0003%. Even considering the larger uncertainty value of 0.06% stated in the literature, the overall uncertainty  $U_{P_{max}}$  equals

$$U_{P_{max}} = 2 \left[ \left( \frac{0.24}{\sqrt{3}} \right)^2 + \left( \frac{0.25}{\sqrt{3}} \right)^2 + \left( \frac{0.06}{2} \right)^2 + \left( \frac{0.064}{\sqrt{3}} \right)^2 + \left( \frac{0.012}{\sqrt{3}} \right)^2 \right]^{0.5} \quad (6)$$

$$= 0.41\%.$$

The uncertainties in  $V_{max}$  and  $I_{max}$  are difficult to assess because of the nonlinear relationship between  $P_{max}$ ,  $V_{max}$  and  $I_{max}$ . A conservative estimate can place  $U_{I_{max}}$  midway between  $U_{I_{sc}}$  and  $U_{P_{max}}$ . Likewise,  $U_{V_{max}}$  can be placed midway between  $U_{V_{oc}}$  and  $U_{P_{max}}$ . Therefore,  $U_{I_{max}} = 0.31\%$  and  $U_{V_{max}} = 0.30\%$ .

The fill factor (FF) is defined as

$$FF = 100 \left( \frac{P_{max}}{V_{oc} I_{sc}} \right) \quad (7)$$

The uncertainty  $U_{FF}$  in FF can be written as

$$U_{FF} = 2 \left[ \left( \frac{U_{P_{max}}}{2} \right)^2 + \left( \frac{U_{V_{oc}}}{2} \right)^2 + \left( \frac{U_{I_{sc}}}{2} \right)^2 \right]^{0.5} \quad (8)$$

assuming that  $V_{oc}$ ,  $I_{sc}$  and  $P_{max}$  are not correlated. This is actually not the case because there is a high degree of correlation between  $P_{max}$  and the other two components, which will tend to reduce the calculated uncertainty. Therefore, this calculation will provide a conservative estimate of  $U_{FF} = 0.56\%$ .

## B.8 Uncertainty in PV Module Back-Surface Temperature

PV module back-surface temperatures are monitored using standard surface mount type T thermocouples. The PV module back-surface temperature uncertainty  $U_{T_{mod}}$  is given in Eqn. (9):

$$U_{T_{mod}} = 2 \left[ \left( \frac{u_{T-Mount}}{\sqrt{3}} \right)^2 + \left( \frac{u_{T-DMM}}{\sqrt{3}} \right)^2 + \left( \frac{u_{TC}}{\sqrt{3}} \right)^2 \right]^{0.5} \quad (9)$$

Rather than being expressed as a percent of reading,  $U_{T_{mod}}$  and other temperature uncertainties are expressed in degrees Celsius. The three elemental components of the temperature uncertainty are  $u_{T-Mount}$  - uncertainty in the mounting and wiring method used in our test bed,  $u_{T-DMM}$ —uncertainty in the instrument measurement of thermocouple channels, and  $u_{TC}$ —uncertainty in the manufacturer specified thermocouple temperature accuracy.

Prior experiments have shown that differences in mounting method can introduce up to a  $u_{T-Mount} = 0.5^\circ\text{C}$  uncertainty in temperature measurement [8]. The remaining two values are based on manufacturer specifications, and are  $u_{T-DMM} = 1.5^\circ\text{C}$  (+50 ppm/ $^\circ\text{C}$  indoor temperature coefficient) and  $u_{TC} = 0.5^\circ\text{C}$ . Therefore,

$$U_{T_{mod}} = 2 \left[ \left( \frac{0.5}{\sqrt{3}} \right)^2 + \left( \frac{1.5}{\sqrt{3}} \right)^2 + \left( \frac{0.5}{\sqrt{3}} \right)^2 \right]^{0.5} \quad (10)$$

$$= 1.9^\circ\text{C}.$$

It should be noted that because this uncertainty is an absolute value, not a percentage of reading, and because the temperature coefficient of measurement is a negligible component of uncertainty (0.05%), the value  $U_{T_{mod}} = 1.9^\circ\text{C}$  remains constant for all measurements of temperature in this experiment configuration.

## B.9 Uncertainty in Irradiance

The irradiance measurement expanded uncertainty  $U_{Irr}$  depends on seven elements –  $u_{Irr-DMM}$  the uncertainty in the auxiliary measurement channel of the MT5 data collection unit,  $u_{Irr-Cal}$  the standard uncertainty of the pyranometer calibration,  $u_{Irr-Angle}$  the uncertainty in coplanar mounting of the pyranometer with the PV module under test, and  $u_{Irr-Tcoef}$  the uncertainty based on outdoor temperature dependence of the pyranometer. Three additional elemental uncertainties are the linearity and stability of the pyranometer and the Type A zero offset due to infrared emissivity. These elemental uncertainties are shown below in Eqn. (11):

$$U_{Irr} = 2 \left[ \left( \frac{u_{Irr-DMM}}{\sqrt{3}} \right)^2 + \left( \frac{u_{Irr-Cal}}{\sqrt{3}} \right)^2 + \left( \frac{u_{Irr-Angle}}{\sqrt{3}} \right)^2 + \left( \frac{u_{Irr-Tcoef}}{\sqrt{3}} \right)^2 + \left( \frac{u_{Irr-Lin}}{\sqrt{3}} \right)^2 + \left( \frac{u_{Irr-Stab}}{\sqrt{3}} \right)^2 + \left( \frac{u_{Irr-TypeA}}{\sqrt{3}} \right)^2 \right]^{0.5} \quad (11)$$

The calculation for  $u_{Irr-DMM}$  follows closely to the uncertainty for voltage uncertainty. For this calculation a representative irradiance of  $600 \text{ W/m}^2$  is assumed. This value, combined with the pyranometer calibration constant of  $9.02 \text{ } \mu\text{V}/(\text{W/m}^2)$ , yields a measurement of  $4.5 \text{ mV}$ , which occurs at a higher measurement range ( $0.05 \text{ V}$ ) of the MT5 unit. The accuracy of the MT5 auxiliary channel on the  $50 \text{ mV}$  range is  $0.2\% + 0.04\%$ . With  $u_{Irr-DMM} = ([\%reading + temperature\ correction] + [\%range + temp.\ correction])$  the calculation is:

$$u_{Irr-DMM} = 100 * \{[(0.2 + (31.76-25)*0.005)*0.01*0.0045] + [(0.04+(31.76-25)*0.005)*0.01*0.05]\} / 0.0045$$

$$u_{Irr-DMM} = 1.0\%.$$

The  $U_{Irr-Cal}$  calibration value for the CM22 pyranometer is determined during NREL's annual pyranometer calibration – BORCAL. The expanded uncertainty for a single calibration value assumed at  $45^\circ$  incidence angle is reported as (for example, using S/N 100163)  $+1.67\% / -1.75\%$ . This value is calculated for incidence angles greater than  $30.0^\circ$  and less than  $60.0^\circ$ . A plot showing the type B elemental uncertainty for this instrument is given in Figure B-2a showing its dependence on incidence angle (labeled here as zenith angle). Calibration data are taken at ambient outdoor temperature, and do not account for the temperature dependence of the pyranometer. Additional uncertainty in translating this horizontal calibration to a tilted-angle calibration is neglected.

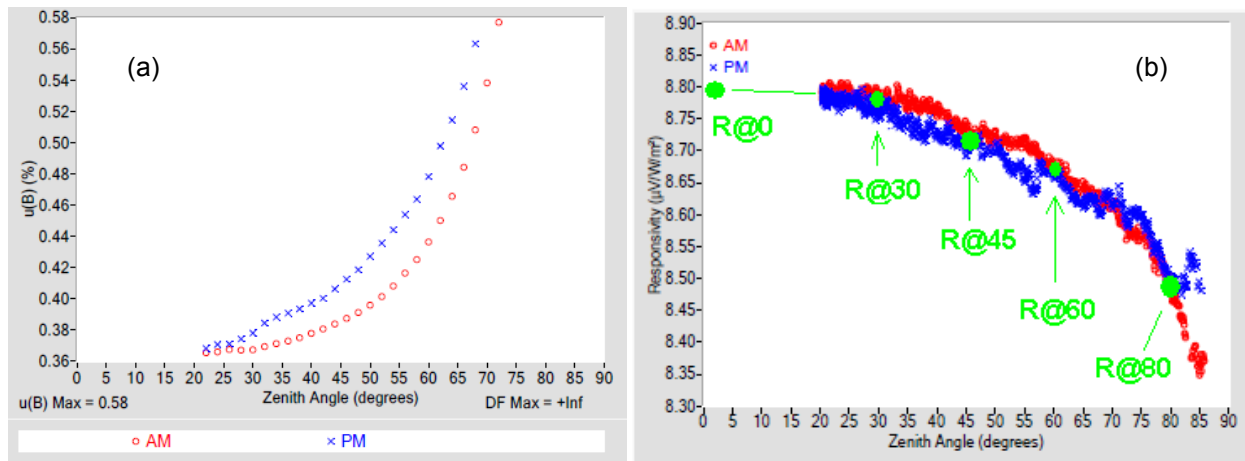


**Figure B-2. a) Type-B standard uncertainty vs. zenith angle for horizontally mounted CM22 (serial # 100163). b) Instrument responsivity ( $\mu\text{V} / \text{Wcm}^2$ ) vs. incidence angle (degrees) (serial # 100163)**

Relevant responsivity values are labeled at 0, 30, 45, 60 and 80 degrees.

A lower calibration uncertainty can be obtained by correcting for incidence angle using a spline fit to Figure B-2, but the calculation considered here assumes the maximum uncertainty for a single  $R_{45^\circ}$  calibration value in the range of  $30.0^\circ - 60.0^\circ$ . According to the uncertainty analysis

of the BORCAL, the calibration uncertainty is a function of the maximum type B uncertainty, which occurs at 60° and the offset uncertainty. According to Figure B-2a, maximum type B elemental uncertainty at 60° in the afternoon is  $u(B)_{60} = 0.48\%$ . The offset uncertainty can be seen in Figure B-2b, which is the difference in response between using a calibration value at 45° and the expected response at 30° or 60°. The elemental offset uncertainty in this case is +0.73 / -0.81%. Combining these elemental values and multiplying by coverage factor  $k = 1.96$ , we arrive at the expanded uncertainty of calibration:  $U_{Irr-Cal} = 1.75\%$ , which is valid in the range of 30° – 60°.

A second uncertainty analysis is required for incidence angles outside of the valid BORCAL angle range of 30° – 60°. For incidence angle conditions outside of this range, an extrapolation of the type-B elemental uncertainty in Figure B-2a and responsivity in Figure B-2b is required. The reason that these error values are not reported during calibration include the fact that small incidence angles are not achieved during the outdoor BORCAL calibration, and the fact that at large incidence angles / low irradiance, there is no traceability to SI standards [9]. An estimate based on manufacturer-specified uncertainty data or extrapolation of calibration data is required. The manufacturer specified incidence angle uncertainty is shown in Figure B-3, which can be considered an upper bound for uncertainty due to incidence angle.

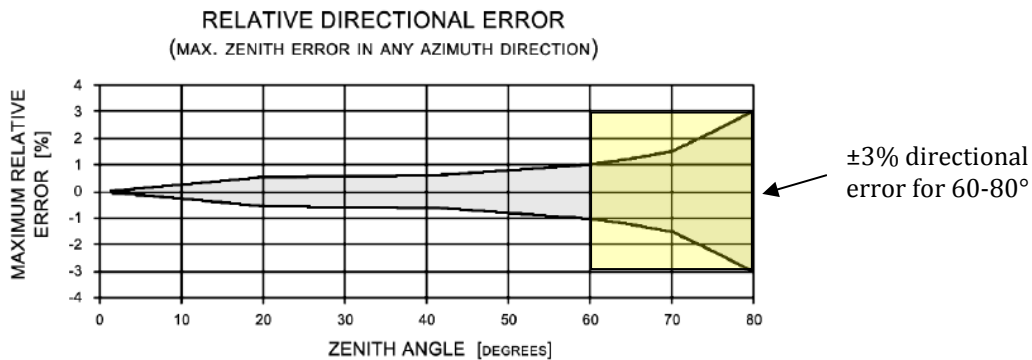


**Figure B-3. Directional error for Kipp & Zonen CMP11 – CMP22 pyranometers [10]**

For low incidence angles below 30°, although BORCAL calibration data for this range do not exist, the directional error in Figure B-3 and the Type B uncertainty in Figure B-2a show decreasing measurement error as incidence angle goes to zero. In addition, the instrument response shown in Figure B-2b shows a trend for responsivity to approach a constant value near 0°. For this reason, the maximum calibration error  $U_{Irr-Cal} = 1.75\%$  is assumed to also apply from zero to 30°.

For large incidence angles of 60° – 80°, the manufacturer data in Figure B-3 shows a type-B expanded uncertainty from directional error of ±3%. This value is combined with the offset uncertainty  $U(off)$  determined during calibration to be 0.54%. The sum of these values (=3.54%) is substituted for  $U_{Irr-Cal}$  to apply during incidence angles up to 80°.

$u_{Irr-Angle}$  is an uncertainty component due to the pyranometer not being exactly coplanar with the solar module. Because the pyranometer output will vary with  $\cos(\alpha)$  where  $\alpha$  is the angle of the pyranometer with respect to the sun,  $u_{Irr-Angle}$  will vary with  $\cos(\alpha) / \cos(\alpha')$  where  $\alpha'$  is the

angle of the PV module with respect to the sun. Assuming a maximum difference in angle between the mounted PV panel and the plane-of-array pyranometer of  $0.5^\circ$ ,  $u_{\text{Irr-Angle}} = [1 - \cos(\alpha' + 0.2^\circ) / \cos(\alpha')] * 100$ . For normal incidence ( $\alpha = 0^\circ$ )  $u_{\text{Irr-Angle}} = 0.004\%$ . For larger incidence angle ( $\alpha = 60^\circ$ )  $u_{\text{Irr-Angle}} = 1.5\%$ . In the example considered here,  $\alpha = 60^\circ$  incidence angle is assumed. This elemental uncertainty is the greatest contributor to total uncertainty at large incidence angles, although a more careful analysis could allow this uncertainty to be reduced, because incidence angle effects will only apply to the direct-beam component of irradiance. At low incidence angles when this elemental uncertainty is large, the irradiance is likely to be composed mainly of diffuse irradiance.

$u_{\text{Irr-Tcoef}}$  is the uncertainty in irradiance due to the temperature response of the pyranometer. The temperature dependence of the CMP-22 pyranometer is shown in Figure B-4. Because the temperature curve is bounded by 0.5% in the outdoor ambient temperature range of interest ( $-20^\circ\text{C} - 50^\circ\text{C}$ ), the maximum uncertainty  $U_{\text{Irr-Tcoef}} = 0.5\%$  is used.

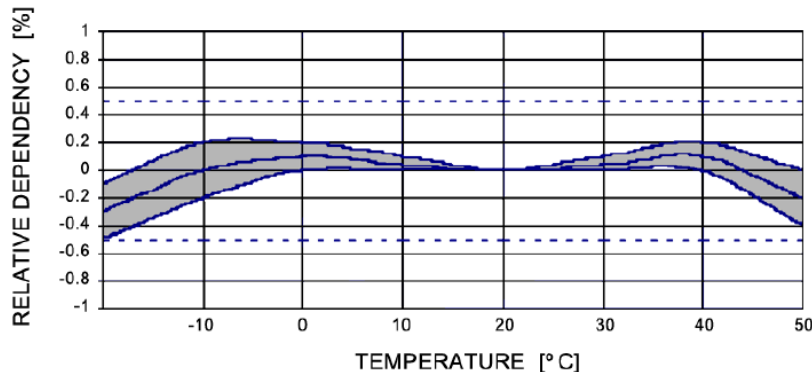


**Figure B-4. Typical temperature dependence of CM22 pyranometer**

Boundary of temperature response in grey

$u_{\text{Irr-Lin}}$  is the stated linearity of the pyranometer in the irradiance range of interest:  $0 - 1,500 \text{ W/m}^2$ . The manufacturer specification sheet lists 0.2% linearity from  $0 - 1,000 \text{ W/m}^2$ . In order to extend this value to the range of interest, both the range and uncertainty are multiplied by 150% to arrive at a linearity of 0.3% from  $0 - 1,500 \text{ W/m}^2$ . This approach is assumed to be valid due to the linearity of the uncertainty value given in the manufacturer’s specifications.

$u_{\text{Irr-Stab}}$ , the manufacturer’s stated annual stability of the pyranometer, = 0.5%. This also includes estimated calibration stability throughout the year, for instance including the pyranometer’s seasonality or daily variation in response.

$u_{\text{Irr-TypeA}}$  is a zero-offset error due to the far-infrared response of the pyranometer dome, creating a temperature difference between the sensor and the outer dome. This results in a particular response to net far-infrared radiation. This uncertainty is stated as a fixed offset value by the manufacturer at  $<3 \text{ W/m}^2$ .

Given these uncertainty components and at a solar incidence angle of  $30.0^\circ$  and a measured irradiance of  $500 \text{ W/m}^2$ :

$$U_{Irr} = 2 \left[ \left( \frac{1.05}{\sqrt{3}} \right)^2 + \left( \frac{1.75}{2} \right)^2 + \left( \frac{0.51}{\sqrt{3}} \right)^2 + \left( \frac{0.5}{\sqrt{3}} \right)^2 + \left( \frac{0.3}{\sqrt{3}} \right)^2 + \left( \frac{0.5}{\sqrt{3}} \right)^2 + \left( \frac{0.6}{\sqrt{3}} \right)^2 \right]^{0.5} \quad (12)$$

$$\mathbf{U}_{Irr} = 2.4\%.$$

For the extended angle range 60.1° – 80.0°, at a solar incidence angle of 80.0° and a measured irradiance of 50 W/m<sup>2</sup>:

$$U_{Irr} = 2 \left[ \left( \frac{1.38}{\sqrt{3}} \right)^2 + \left( \frac{3.54}{2} \right)^2 + \left( \frac{5.0}{\sqrt{3}} \right)^2 + \left( \frac{0.5}{\sqrt{3}} \right)^2 + \left( \frac{0.3}{\sqrt{3}} \right)^2 + \left( \frac{0.5}{\sqrt{3}} \right)^2 + \left( \frac{6}{\sqrt{3}} \right)^2 \right]^{0.5} \quad (13)$$

$$\mathbf{U}_{Irr\_60-80} = 9.8\%.$$

Several possible contributors to uncertainty were neglected in this analysis. Irradiance was assumed to be constant over the measurement plane, including the pyranometer and PV modules under test. This is likely the case under clear-sky conditions, but may not be the case under rapidly changing irradiance conditions, for example, due to cloud cover.

Additionally, irradiance is assumed to be constant during the approximate second required to measure an I-V curve. This is not always the case, and this uncertainty is mitigated by measuring irradiance both before and after a curve is taken. Curves taken under variable conditions, defined as irradiance changing by more than 5 W/m<sup>2</sup> (as measured by a fast-response LI-COR photodiode), are flagged to be excluded from the dataset.

For mPERT, three additional irradiance measurements are collected using a CR1000 datalogger: direct normal irradiance, diffuse horizontal, and global horizontal. Several minor differences exist in the calculation of uncertainty for these values.

For all measurements, U<sub>Irr</sub>-DMM is based on the analog input characteristics of the CR1000 datalogger rather than the MT5. The CR1000 has a stated accuracy specification of 0.06% of reading + resolution error. The resolution error depends on the measurement range: 1.33 μV for the 2.5-mV range, 2μV for the 7.5-mV range, and 4.33 μV for the 25-mV range. These accuracy specifications are valid for an indoor ambient temperature range of 0°C – 40°C with no additional temperature-based correction.

Specifically, for the measurement of direct normal irradiance, the device is placed on a two-axis tracker and kept pointed at the sun. The acceptance angle of the instrument is 0.75 degrees, with zero uncertainty assumed from pointing error so long as the instrument is mounted within this window. Additionally, Type A near-IR error is zero for this instrument. The accuracy of the calibration of this instrument is valid within a zenith angle of 0 to 72 degrees.

For global horizontal irradiance, the tilt angle error is that between the pyranometer and level. Based on the uncertainty of the bull's eye spirit level, this error is 0.1 degree. Other calculations remain the same as for POA irradiance.

Diffuse horizontal irradiance does not depend on the solar position because the sun disc is shaded for this measurement. Therefore, tilt error is assumed to be zero. All other calculations remain the same.

## B.10 Uncertainty in Outdoor Ambient Temperature, RH, Pressure, and Precipitation

The WXT520 meteorological sensor has other meteorological sensors, including ambient (dry bulb) temperature, relative humidity, barometric (atmospheric) pressure, and precipitation.

Ambient temperature is measured with an integrated air temperature sensor. The stated accuracy of the sensor is given in its user’s manual in Figure B-5, in terms of degrees C:

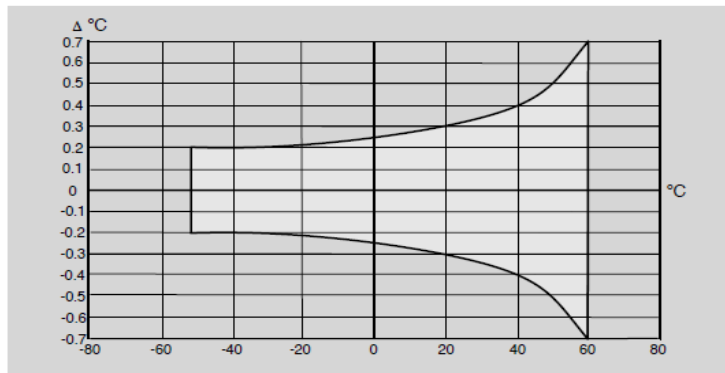


**Figure B-5. Temperature uncertainty (°C) of outdoor ambient temperature sensor**

The uncertainty has a minimum of  $\pm 0.2^{\circ}\text{C}$  at low temperatures ( $-50^{\circ}\text{C}$ ) and increases to  $\pm 0.7^{\circ}\text{C}$  at  $60^{\circ}\text{C}$  ambient. A third-order polynomial was fit to the calibration values, which approximates this calibration shape (Figure B-6). The equation is:

$$\Delta T[\text{C}] = 1.3 \times 10^{-6} T^3 + 4.3 \times 10^{-5} T^2 + 4.7 \times 10^{-5} T + 0.257$$

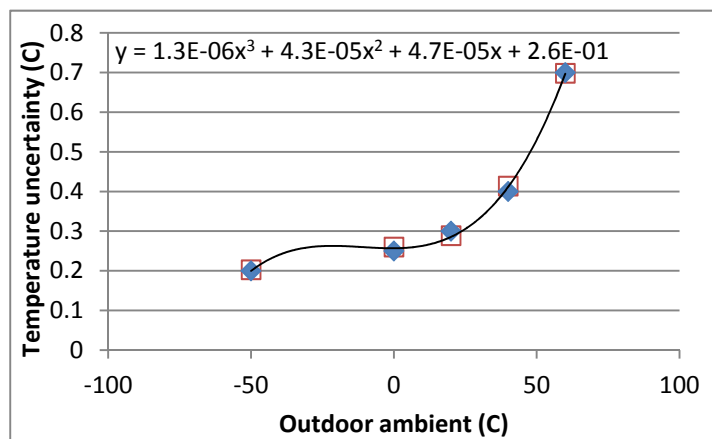


**Figure B-6. Third-order polynomial fit to outdoor ambient temperature uncertainty**

Actual calibration points are filled diamonds, calculated values are open squares.

The calculation of outdoor ambient temperature is simply a function of the calibrated temperature uncertainty at the appropriate outdoor temperature:

$$U_{T_{amb}} = 2 \left[ \left( \frac{u_{T_{amb-Cal}}}{\sqrt{3}} \right)^2 \right]^{0.5}$$

For the specific condition of outdoor ambient = 30°C, the overall uncertainty (in degrees C) is:

$$U_{T_{amb}} = 2 \left[ \left( \frac{0.332}{\sqrt{3}} \right)^2 \right]^{0.5}$$

$$U_{T_{amb}} = 0.383^\circ \text{ C.}$$

The next meteorological parameter monitored by the WXT520 is relative humidity. The stated RH accuracy spec (in terms of percent relative humidity) is  $\pm 3\%$ RH for RH from 0%–90%, and  $\pm 5\%$ RH for relative humidity from 90%–100%. For a moderate value of RH (<90%RH), the uncertainty is:

$$U_{RH} = 2 \left[ \left( \frac{3}{\sqrt{3}} \right)^2 \right]^{0.5}$$

$$U_{RH} = 3.46 \% \text{RH.}$$

The next meteorological parameter is barometric pressure. This is a temperature-dependent calculation, with a stated accuracy of 0.5 mb (hPa) for outdoor ambient temperature in the range of 0°C – 30°C, and 1.0 mb (hPa) for outdoor ambient temperature from -52°C – 60°C. For the typical barometric conditions of 1,013 mb at 30°C, the calculation for uncertainty in pressure (as a percentage) is:

$$U_{Press} = 2 \left[ \left( \frac{1/1013 * 100}{\sqrt{3}} \right)^2 \right]^{0.5}$$

$$U_{Press} = 0.11 \%.$$

The final meteorological measurement provided by the WXT520 is accumulated precipitation in millimeters. The stated accuracy of this value is 5%, with the caveat that spatial variation and wind-driven effects are not accounted in this value. With the translation from a 1.73 coverage factor to a Gaussian coverage factor, the overall uncertainty is:

$$U_{Precip} = 5.77 \%$$

## B.11 References

1. ASTM Standard E1036. *Standard Test Methods for Electrical Performance of Nonconcentrator Terrestrial Photovoltaic Modules and Arrays Using Reference Cells*. ASTM International, West Conshohocken, PA.
2. International Organization for Standardization. *Guide to the Expression of Uncertainty in Measurement*. ISO: Geneva, 1995, ISBN 92-67-10188-9.
3. Taylor, B.N.; Kuyatt, C.E. *Guidelines for Evaluating and Expressing the Uncertainty of NIST Measurement Results*. NIST Technical Note 1297, 1994.
4. Adams, T.M. *G104-A2LA Guide for Estimation of Measurement Uncertainty in Testing*. A2LA Technical Guidance Report G104, 2002. Accessed October 6, 2011: [http://www.a2la.org/guidance/est\\_mu\\_testing.pdf](http://www.a2la.org/guidance/est_mu_testing.pdf)
5. Natrella, M.G. *Experimental Statistics*. National Bureau of Standards Handbook 91, p. 5–34. August 1, 1963, reprinted October 1966.
6. Whitfield, K.; Osterwald, C.R. “Procedure for Determining the Uncertainty of Photovoltaic Module Outdoor Electrical Performance.” *Prog. Photovolt.* (9), 2001; pp. 87–102.
7. Emery, K. *Uncertainty Analysis of Certified Photovoltaic Measurements at the National Renewable Energy Laboratory*. NREL Technical Report TP-520-45299, August 2009.
8. Smith, R.; Kurtz, S.; Sekulic, B. “Back-of-Module Temperature Measurement Methods.” *Solar Pro* 4.6, 2011; p. 90.
9. Adams, T.M. *G104- A2LA Guide for Estimation of Measurement Uncertainty in Testing*. A2LA Technical Guidance Report G104, 2002. Accessed October 6, 2011: [http://www.a2la.org/guidance/est\\_mu\\_testing.pdf](http://www.a2la.org/guidance/est_mu_testing.pdf) on 10/6/11.
10. Natrella, M.G. *Experimental Statistics*. National Bureau of Standards Handbook 91. 1963.

## Appendix C – Sample Read Statements

This appendix contains code snippets in C# for reading the header and data lines.

### C.1 Reading the Header Line

Line 2 of the data file contains the header information. The line is read as a string and then split or parsed into an array of strings. The string array is dimensioned beginning with zero; consequently, the element field numbering in Table 3-2 is one greater than the corresponding string array offset. String array values are converted to a numeric value as appropriate. Example code with comments (in green) is shown below.

```
string strLine = sr.ReadLine();           // Reads a line of data into the string
                                           // variable strLine.

string[] strArray = strLine.Split(',');    // Splits or parses line of data
                                           // into array of string variables

                                           // Assign array variables to header elements listed in Table 3-2

string PVid = strArray[0];                 // PV Module Identifier
string city = strArray[1];                 // City
string state = strArray[2];                // State
int    tz = Convert.ToInt32(strArray[3]);  // Time Zone
double lat = Convert.ToDouble(strArray[4]); // Latitude
double lng = Convert.ToDouble(strArray[5]); // Longitude
double elev = Convert.ToDouble(strArray[6]); // Elevation
double pvTilt = Convert.ToDouble(strArray[7]); // PV Module Tilt
double pvAzm = Convert.ToDouble(strArray[8]); // PV Module Azimuth
```

### C.2 Reading the Data Lines

Data lines begin with line 4 and continue until the end of the file. Like the header line, the lines are read as strings and then split or parsed into an array of strings. Again, the string array is dimensioned beginning with zero; consequently, the element field numbering in Table 3-3 is one value greater than the corresponding string array offset. String array values are converted to a numeric value as appropriate. Example code is shown below. Data lines are variable length due to the presence of the I-V curve data, which varies in the number of data points depending on conditions under which it is measured. The value of N is used to determine how many current-voltage pairs of the I-V curve are present.

```

string strLine = sr.ReadLine(); // Reads a line of data into the string
                                // variable strLine.

string[] strArray = strLine.Split(','); // Splits or parses line of data
                                        // into array of string variables

// Parse the Time into a date and time of day

string[] strArray2 = strArray[0].Trim().Split('T');
string[] strArray3 = strArray2[0].Split('-'); // Parse the date

int year = Convert.ToInt32(strArray3[0]); // Year
int month = Convert.ToInt32(strArray3[1]); // Month
int day = Convert.ToInt32(strArray3[2]); // Day

strArray3 = strArray2[1].Split(':'); // Parse the time

int hour = Convert.ToInt32(strArray3[0]); // Hour
int minute = Convert.ToInt32(strArray3[1]); // Minute
int second = Convert.ToInt32(strArray3[2]); // Second

// Assign Data Elements

double poaCMP = Convert.ToDouble(strArray[1]); // POA Irradiance
double poaCMPunc = Convert.ToDouble(strArray[2]); // POA Irradiance Uncertainty

double Tpv = Convert.ToDouble(strArray[3]); // PV Module Back-Surface
                                                // Temperature
double TpvUnc = Convert.ToDouble(strArray[4]); // PV Module Back-Surface
                                                // Temperature Uncertainty

double isc = Convert.ToDouble(strArray[5]); // PV Module Isc
double iscUnc = Convert.ToDouble(strArray[6]); // PV Module Isc Uncertainty

double pmp = Convert.ToDouble(strArray[7]); // PV Module Pm
double pmpUnc = Convert.ToDouble(strArray[8]); // PV Module Pm Uncertainty

double imp = Convert.ToDouble(strArray[9]); // PV Module Imp
double impUnc = Convert.ToDouble(strArray[10]); // PV Module Imp Uncertainty

double vmp = Convert.ToDouble(strArray[11]); // PV Module Vmp
double vmpUnc = Convert.ToDouble(strArray[12]); // PV Module Vmp Uncertainty

double voc = Convert.ToDouble(strArray[13]); // PV Module Voc

```

```

double vocUnc = Convert.ToDouble(strArray[14]); // PV Module Voc Uncertainty
double ff = Convert.ToDouble(strArray[15]); // PV Module FF
double ffUnc = Convert.ToDouble(strArray[16]); // PV Module FF Uncertainty
double poaCMPdelta = Convert.ToDouble(strArray[17]); // Delta CMP 22 POA
double poaLICORdelta = Convert.ToDouble(strArray[18]); // Delta LI-COR POA
double mt5Temp = Convert.ToDouble(strArray[19]); // MT5 Cabinet Temperature
double dryBulbTemp = Convert.ToDouble(strArray[20]); // Dry Bulb Temperature
double dryBulbTempUnc = Convert.ToDouble(strArray[21]); // Dry Bulb
// Temperature Uncertainty
double rh = Convert.ToDouble(strArray[22]); // Relative Humidity
double rhUnc = Convert.ToDouble(strArray[23]); // Relative Humidity
// Uncertainty
double pres = Convert.ToDouble(strArray[24]); // Atmospheric Pressure
double presUnc = Convert.ToDouble(strArray[25]); // Atmospheric Pressure
// Uncertainty
double precip = Convert.ToDouble(strArray[26]); // Precipitation
double dn = Convert.ToDouble(strArray[27]); // Direct Normal Irradiance
double dnUnc = Convert.ToDouble(strArray[28]); // Direct Normal Irradiance
// Uncertainty
double dnSD = Convert.ToDouble(strArray[29]); // Direct Normal Irradiance
// Standard Deviation
double gh = Convert.ToDouble(strArray[30]); // Global Horizontal Irradiance
double ghUnc = Convert.ToDouble(strArray[31]); // Global Horizontal Irradiance
// Uncertainty
double ghSD = Convert.ToDouble(strArray[32]); // Global Horizontal Irradiance
// Standard Deviation
double df = Convert.ToDouble(strArray[33]); // Diffuse Horizontal Irrad.
double dfUnc = Convert.ToDouble(strArray[34]); // Diffuse Horizontal Irrad.
// Uncertainty
double dfSD = Convert.ToDouble(strArray[35]); // Diffuse Horizontal Irrad.
// Standard Deviation
double solarQA = Convert.ToDouble(strArray[36]); // Solar QA Residual

```

```

double soilDerate = Convert.ToDouble(strArray[37]); //PV Module Soiling Derate

strArray2 = strArray[38].Split(':'); // Parse the Start Time

int startMaintHour = Convert.ToInt32(strArray2[0]); // Hour of Daily Maint-
// enance Start Time

int startMaintMinute = Convert.ToInt32(strArray2[1]); //Minute of Daily Maint-
// enance Start Time

strArray2 = strArray[39].Split(':'); // Parse the End Time

int endMaintHour = Convert.ToInt32(strArray2[0]); // Hour of Daily Maint-
// enance End Time

int endMaintMinute = Convert.ToInt32(strArray2[1]); // Minute of Daily Maint-
// enance End Time

double precipPriorMaint = Convert.ToDouble(strArray[40]); // Precipitation
// Prior to Daily Maintenance

int nData = Convert.ToInt32(strArray[41]); // Number of I-V Curve Data Pairs
// Note: number of remaining fields depends on value of nData

double[] amps = new double[nData], volts = new double[nData];

// Convert string values to current-voltage pairs

for (int i = 0; i < nData; i++)
{
    amps[i] = Convert.ToDouble(strArray[42 + i]); // I-V Curve I Values
    volts[i] = Convert.ToDouble(strArray[42 + nData + i]); // I-V Curve V Values
}

```